Biofilament interacting with molecular motors

by

Janusz Martin Meylahn

Thesis presented in partial fulfilment of the requirements for the degree of Master of Science in Theoretical Physics in the Faculty of Science at Stellenbosch University

Department of Physics,
University of Stellenbosch,
South Africa.

Supervisor: Prof. K. K. Müller-Nedebock and Prof. H. Touchette

December 2015

Declaration

By submitting this thesis electronically, I declare that the entirety of the work contained therein is my own, original work, that I am the sole author thereof (save to the extent explicitly otherwise stated), that reproduction and publication thereof by Stellenbosch University will not infringe any third party rights and that I have not previously in its entirety or in part submitted it for obtaining any qualification.

Abstract

Biofilament interacting with molecular motors

J. M. Meylahn

Department of Physics,
University of Stellenbosch,
South Africa.

Thesis: MSc (ThP)

September 2015

We study molecular motors moving along a filament or polymer using two different mathematical models in which motors are idealised as springs. In the first model we study the average and the fluctuations of the motor stretch by modelling the motion of the motors along the filament using a simple stochastic differential equation with linear friction. We use the notion of stochastic resetting to explicitly include the attachment and detachment dynamics of the motors to and from the filament and study the fluctuations around the most probable value of the mean stretch using methods from large deviation theory. The second model uses methods from field theory to model a dynamic network consisting of a single polymer and many molecular motors. In this case, we develop techniques to include the bias motion of the molecular motors in a weighting factor for the formation of specific networks rather than in the dynamical constraints of the partition function which allows us to study the steady-state of the network using a self-consistency argument and a saddle-point approximation.

Uittreksel

Biofilament interaksie met molekulare motore

("Biofilament interacting with molecular motors")

J. M. Meylahn

Departement Fisika,
Universiteit van Stellenbosch,
Suid Afrika.

Tesis: MSc (ThP)

September 2015

Ons beskou twee wiskundige modelle vir molekulêre motore wat langs 'n filament of polimeer beweeg. Die motore word as vere geïdealiseer. In die eerste model bestudeer ons die gemiddelde uitrekking van die motor, asook die fluktuasies in die uitrekking, deur die beweging van die motor met 'n eenvoudige stogastiese differensiaalvergelyking met lineêre wrywing te beskryf. Ons gebruik stogastiese hersetting om eksplisiet die aanheg en ontkoppeling dinamika van die motore aan die filament te modelleer en bestudeer dan die fluktuasies rondom die mees waarskynlike waarde van die gemiddelde uitrekking met metodes uit groot-afwykingsteorie. Die tweede model maak gebruik van metodes uit veldeteorie om 'n dinamiese netwerk van een polimeer en 'n aantal molekulêre motore te beskryf. Hier ontwikkel ons tegnieke om die voorkeur beweging van die motore deur 'n gewigsfaktor vir die vorming van spesifieke netwerke te bewerkstellig, eerder as om dit dinamies in die partisiefunksie af te dwing. Hierdie benadering laat ons dan toe om die bestendige toestand van die netwerk deur 'n selfkonsistensie argument en saalpuntbenadering te bestudeer.

Acknowledgements

I would like to express my sincerest gratitude to my supervisors Prof. Touchette and Prof. Müller-Nedebock for their guidance throughout this research project.

The Harry Crossly Foundation, NITheP and the Physics department in particular Prof. Rohwer, Prof. Schwoerer and Prof. Müller-Nedebock for financial support during my studies.

My fellow students in particular Kevin Li for intense late night discussions on a variety of interesting topics and Ruan Viljoen for laughing with me when I was frustrated or confused.

My office mates Stanard Pachong, Mateyisi Mohau and Chris Rohwer for a pleasant and fruit full work environment.

Lastly my family for supporting me through out my studies. I am forever grateful for your support and love.

Dedications

This thesis is dedicated to my parents Felix and Barbara Meylahn.

Contents

List of Figures

Chapter 1

Introduction

In this thesis we will study different models of molecular motors found in biological cells, which are composed physically of proteins and are responsible for transportation of materials such as chemicals and proteins around the cell. These motors perform their individual tasks by converting chemical energy in the form of ATP into mechanical work. There are many different types of motors and each is optimized to perform a very specific task.

Many models used to describe molecular motors focus on their mean behaviour as well as their steady-state. Here we will study new ways of describing them that are suited to study the mean behaviour as well as the fluctuations around this mean. We will also focus on including the attaching and detaching of the motors to their load explicitly in the models.

In the next sections we will explain in more detail what molecular motors are and give the basic ideas of the models we will study.

1.1 Molecular motors

Molecular motors are machines in cells that perform work. An example of a molecular motor moving along a filament can be seen on the left of Fig. 1.1 and a motor transporting a load is seen on the right.

The study of these motors forms a sub-field of soft active matter. This field studies the statistical and mechanical properties of systems with the shared property that some of their constituents are self-driven. For a component of a system to be self-driven it must produce its own power like a motor. Some examples of soft active matter are biological filaments with molecular motors, the cytoskeleton, suspended bacteria, cell layers, and animal flocks. A good review of soft active matter is given by Marchetti *et al.* [3].

In the case of a molecular motor carrying a load, it is the motor that is self-driven. Motors typically function by the hydrolisis of ATP, which produces energy and ADP and can use this energy to perform tasks such as transporting biological materials, contracting muscles, and powering the beating of flagella

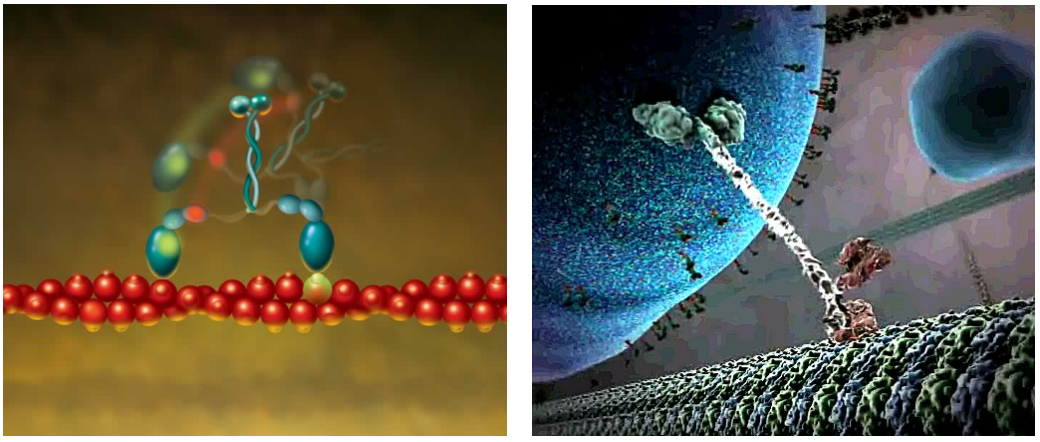

Figure 1.1: (Left) Molecular motor moving along a filament (taken from [1]). (Right) A type of motor called kinesin carrying a load (taken from [2]).

and cilia. Put simply, a molecular motor uses chemical energy from its environment to do work.

Since the load a molecular motor has to carry is normally quite heavy in comparison to the force a molecular motor can exert (on the scale of piconewtons), motors often works in combination. The number of motors involved in the case of muscles contraction, for example, can reach up to 10^{19}. This requires complicated communal coordination which leads to interesting collective dynamical behaviour characterised by oscillations, hysteresis, and dynamical formation of structures [3]. Some recent papers find interesting phenomena like dynamic instabilities [4], bidirectional motion [5] or biased transport in the case where the direction in which the motor moves along the filament is alternating in time [6].

One of the first steps taken towards the description of molecular motors is to classify them as either "rowers" or "porters". Rowers spend most of their time detached from the filament but produce large forces when attached almost like the stroke of a rower. This makes it difficult for them to function independently. Porters on the other hand produce smaller forces and spend a lot of time attached to the filament so that they can operate individually but struggle to cooperate in larger groups. To make this distinction more exact, a motor can be characterised using its duty ratio, which is a measure of the fraction of time the motor spends attached to a filament [7].

In biological cells one typically finds a large variety of molecular motors that are all optimised to perform certain tasks within the cell. This implies that there are many different mathematical descriptions for these motors that depend on the finer details of the inner workings of the motors. A good overview of the various types of motors and the descriptions thereof is given by Guerin *et al* [8].

Many models used to describe molecular motors consider them to be similar to a mechanical spring with spring constant k_M (see Fig. 1.2) and often con-

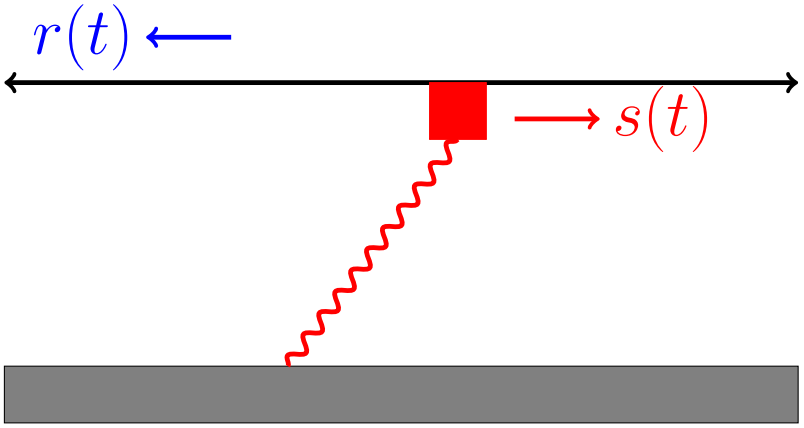

Figure 1.2: Single filament with single motor with $r(t)$ the filament position and $s(t)$ is the motor position relative to the filaments center.

sider one or two dimensional versions [9]. This is because motors often move along filaments or on membranes so that their motions is in those cases really restricted to the dimension of the object they are moving on. These models are often suited to study many motors simultaneously and study properties like the average force exerted by a molecular motor. An alternative to the spring model is the description of molecular motors using a ratchet mechanism [8].

In this thesis we will study models of spring-like motors in one dimension using two different mathematical descriptions. These descriptions will be useful for studying the mean behaviour of many motors in their steady-state, as well as the fluctuations around the mean behaviour. The focus in our study is to characterise the fluctuations explicitly in a stochastic model, which has not been done in detail in the literature. The common theme in our descriptions will be the focus on the statistics of the attaching and detaching of the motors to and from their load. We introduce the models we will study in the next sections.

1.2 Simple two-state model of molecular motors

The first model we will consider is a simple one-dimensional model where the motor switches between two states only, namely, the fully stretched attached state and the detached state. We are interested in including the attachment and detachment dynamics in our description of molecular motors explicitly, in a stochastic way.

The interest for doing this was sparked by a paper written by Banerjee *et al* [9] who found that the collective behaviour of molecular motors changes depending on the relation between the probability of a motor detaching and the motor state. They compare the case where the motor detaches with a constant

rate to the case where the detachment probability depends on the force the motor is exerting on its load. The larger the force the motor is exerting the more likely it is for the motor to detach. The second case makes more sense physically but is more difficult to describe mathematically. These calculations were done using mean-field approximations to include the attachment and detachment dynamics.

To include these dynamics explicitly in a model for the molecular motors we start with a very crude model of molecular motors: it considers the motors to be very stiff springs such that a motor exerts a constant force when it is attached to its load and no force when it is not attached. This means the motor is switching between two states.

With this model we study the average force a motor exerts over time as well as the average force many motors working together would exert as a function of time. The model also allows us to study not just this mean behaviour in time and the case of many motors, but also allows us to characterise the fluctuations around this behaviour in both cases. We do this using techniques from large deviation theory, which is used to study the probability of rare events. The same techniques will be used in Chapter 3, where we will study a more realistic model of molecular motors using resetting. In the next section, we give an introduction to resetting

1.3 Stochastic resetting

Stochastic resetting can be used to study the motion of a molecular motor attached by its tail to a substrate while attaching and detaching to its load. In our case we will consider the load to be a biological filament which the molecular motor moves along by a diffusion process with linear friction.

A motor transporting a filament first attaches to the filament and moves along the filament according to a diffusion process. As it moves, its tail becomes more and more stretched so that the force it exerts on the filament becomes larger. At some point the motor detaches from the filament and returns to its initial state where it is not stretched.

Stochastic resetting in the context of molecular motors is essentially a modification to the diffusion process to include this last step of the motor detaching, relaxing and reattaching. The modification consists of including the probability of the motor being instantaneously moved to its initial position in the diffusion process. This means that the diffusion process is restarted at any point in time with a certain probability. We show a visualisation of the process in Fig. 1.3.

The phenomenon of stochastic resetting hs only recently received attention in the literature and has been explored mainly in the context of search strategies [10]. This is motivated by the common experience of searching for your keys. You start searching at the point where you last saw them and if you do

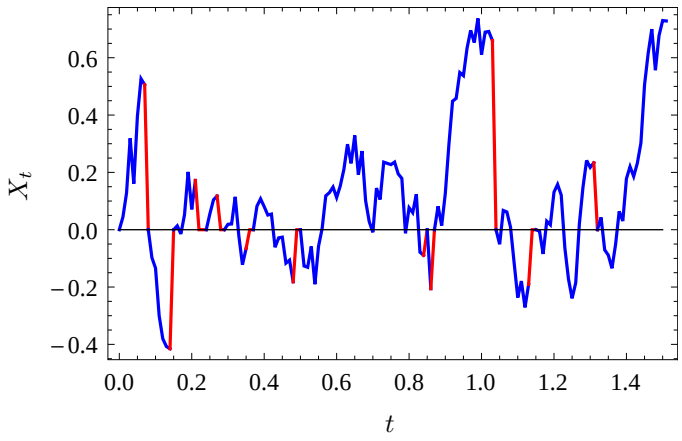

Figure 1.3: Visualisation of a diffusion process X_t with resetting steps in red where X_t returns to the origin at random times.

not find them after a certain amount of time you tend to return to the place where you started.

There are many other examples where resetting is applicable. An animal searching for food, for example, usually involves a local search around a specific area and after a while a larger non-local move to a new area or back to its nest [11; 12; 13]. Search algorithms in computer science can also be optimised using random walks with resetting in the context of hard combinatorial problems [14; 15; 16]. In biology certain organisms use resetting to adapt to different environments by switching between different phenotypic states [17; 18; 19; 20; 21]. A discrete version of what we call resetting has been studied extensively in the context of birth and death processes with catastrophes. These studies model the growth of a population that is repeatedly hit by a catastrophe that wipes out a large part of the population, essentially "resetting" the population to a new size almost instantaneously [22; 23; 24].

We are interested in applying the idea of stochastic resetting to the motion of molecular motors to explicitly include the resetting dynamics after a motor detaches. Using large deviation theory we will be able to study the most probable value of the average force exerted by a molecular motor in time as well as to characterise the fluctuations around it.

1.4 Polymer network models

In our second approach to studying molecular motors we will study a polymer network consisting of many molecular motors attaching and detaching from one filament. A polymer network consists of many biological filaments or *polymers* that are physically linked to each other by proteins called *cross-links*. We will do this using techniques developed for studying networks that change in time. The majority of this section will follow the introduction to polymers given by

Karl Möller [25].

The study of networks of biopolymers has been motivated largely by the applicability of the models to real networks such as the cytoskeleton which is responsible for the mechanical properties of cells and serves as a sort of rail track system for transport processes in cells. Many of these models for polymer networks are becoming experimentally accessible.

Theorists classify the different filaments or polymers that can be involved in creating a network into three categories, namely flexible, semi-flexible and stiff. To formalise these categories we introduce the idea of the persistence length which is the distance along a polymer over which the orientation of polymers segments becomes uncorrelated. If the contour length of the polymer is large in comparison with the persistence length the polymer is classified as being flexible. These are typically the easiest polymers to deal with but are not always realistic. If the persistence length is comparable to the contour length the polymer is semi-flexible. Most polymers in biology are of this type and much work has gone into modelling networks consisting of these. Lastly stiff polymers have a persistence length much longer than the contour length. These polymers can be thought of as stiff rods. Each of these classes requires a different theoretical description and much work has gone into developing sensible models for the different types of polymers. Notable contributions are due to Doi and Edwards [26].

The next step in describing polymer networks is to introduce cross-linking. A cross-link could, for example, be permanently attaching two positions along a polymer to each other. This would be a permanent cross-link and is the sort of cross-linking that takes place when manufacturing rubbers. Alternatively a cross-link could be dynamic so that the position at which two polymers are connected changes in time according to an evolution equation. This is the sort of cross-link we will use to describe a molecular motor attaching, moving along and detaching from a filament.

We will study a dynamic network of molecular motors and a filament. Our approach will include the attachment and detachment of the motors not in the dynamics of the motors as in the previous section but in the dynamic formation of networks.

1.5 Outline of thesis

This thesis is composed of two different parts. The first part includes Chapters 2 and 3 and the second Chapters 4 and 5.

In Chapter 2 we study the mean behaviour as well as fluctuations of a simple two state model for molecular motors using large deviation theory. The two-state model is a crude approximation of a molecular motor and is physically relevant in the limit of motors with a very stiff tail. The simplicity of the model allows us to study the fluctuations of the behaviour of a single

motor in time as well as those of many non-interacting motors cooperating to transport a filament.

Following this, in Chapter 3, we study the average stretch in time of a molecular motor undergoing a diffusion process with stochastic resetting and characterise the dominant behaviour of this random variable as well as the fluctuations around it. This can be used to describe a single molecular motor transporting a filament. With this model we come closer to describing the realistic motion of a molecular motor than the in the model of the previous chapter because we include the stochastic motion of the motor along the filament.

The second part of the thesis starts with an introduction to the methods needed for a theory of dynamic networks in Chapter 4. We use these methods in Chapter 5 to study a network consisting of many molecular motors attached, by their tails, to a fixed ring while transporting another larger filamentous ring by attaching, diffusing along and detaching from it. We do this using techniques from field theory developed to study dynamic polymer networks. Here the attaching and detaching of the motors is modelled not by resetting but by letting the network of motors with the filament reform at each point in time.

In the last chapter we conclude the thesis by summarising our findings, contextualising our work and listing possible extensions and open questions regarding the work of the thesis.

Part I

Chapter 2

Collective behaviour of independent motors

In this chapter we study the attachment and detachment dynamics of individual motors to and from a filament. We consider the motors to be stiff and our focus will be on studying the mean behaviour as well as the fluctuations in the long time and many motor limit. We will characterise fluctuations close to the typical behaviour as well as those far from it.

Some work similar to that of this chapter was done on hierarchical stochastic processes under the name of random evolutions [27; 28; 29; 30]. The application to molecular motors and the use of large deviation theory is however novel.

2.1 Simulation for response diagram

The model of molecular motors that we consider is illustrated in Fig. 1.2 and is described by the following coupled Langevin equations

$$\mu_{\mathrm{f}}\dot{r} = F_{\mathrm{ext}} - k_{\mathrm{s}}(s+r) + \eta_{\mathrm{f}} \tag{2.1.1}$$

$$\mu_{\mathrm{m}}\dot{s} = f_{\mathrm{s}} - k_{\mathrm{s}}(s+r) + \eta_{\mathrm{m}}. \tag{2.1.2}$$

Here, the position of the filament is $r(t)$ with regards to the origin and the position of the motor, $s(t)$ is with respect to the center of the filament. Additionally we have the spring constant k_{s}, the noise for the motor and filament respectively η_{m} and η_{f}, the drag coefficients for the motor and filament respectively μ_{m} and μ_{f}, the external force applied to the filament, F_{ext} and the stall force for the motor, f_{s}.

In this chapter we will neglect both η_{m} and η_{f} which means that a motor attaches and moves along the filament deterministically until its tail, which is attached to a fixed position, is stretched to such a degree that the force it exerts on the filament is equal to the stall force f_s. At this point the motor "stalls" and stops moving.

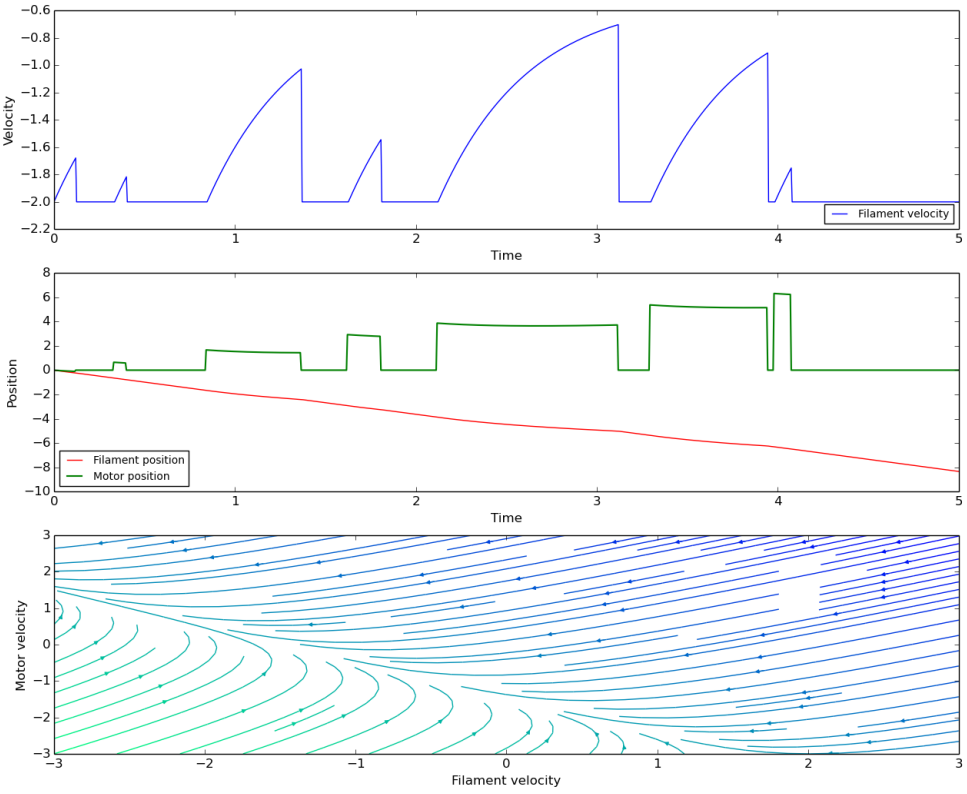

Figure 2.1: A typical process of Eqs. (2.1.1) and (2.1.2) Top - Filament velocity in time, Middle - Motor position along the filament in time, Bottom - Vector field for motor and filament velocity.

A typical process described by Eqs. (2.1.1) and (2.1.2) without noise can be seen in Fig. 2.1. Here we have included the attaching and detaching in the simulation, which is not part of the Langevin model. The velocity depicted in the first block of the figure is the filaments velocity. We see that as the motor attaches it is not stretched. It starts moving along the filament, becoming more and more stretched and starts pulling the filament. The reason for the discrete jumps in the second part of the figure is that the motor position is zero when detached and a position relative to the center of the filament when attached. This means the second time it attaches it is no longer attaching at the position given by zero along the filament. The third block in Fig. 2.1 shows the flow field of filament and motor velocity. We see that the system will take some time to flow to the steady state depending on the initial values of the motor and filament velocities.

Even though the motor evolves deterministically along the filament, there is still an element of randomness in the model, given by the detachments and

reattachments of the motor. The question is now what the probability of detaching depends on. In many studies it is taken to be a constant rate r, so that the probability of detaching in a time interval Δt is $r\Delta t$. In reality, however, the bigger the stretch of the motor the more likely it is for the motor to detach. This means that the probability should be a function of the motor stretch.

In [9], Banerjee *et al.* investigate how a system consisting of many motors moving along a filament changes its behaviour when a stretch-dependent detachment rate is introduced. The stretch dependent function used is a polynomial of second order in the stretch (x from now on) but the exponential of x is mentioned as a more realistic function. After a mean-field approximation for the attachment times and the number of attached motors, they predict a phase transition and hysteresis behaviour in the response of the system described by the steady-state velocity of the filament obtained for a given applied force F_{ext}. They obtain this prediction for a detachment rate that is a polynomial of second order in x; for a constant detachment rate the response is linear.

We simulated the coupled Langevin equations from Eqs. (2.1.1) and (2.1.2) for many motors with noise and introduced the attachment and detachment dynamics with a variable functional dependence on the stretch to reproduce the steady-state velocity versus external force curve or response diagram found in [9]. The aim is to see if the actual model with an x-dependent detachment probability shows the same behaviour found in the mean-field calculation. We repeated the simulation for different values of the external force and let the system evolve until it reached a steady-state velocity for each of them. The results for a constant detachment rate and an exponential stretch dependence can be seen in Fig. 2.2.

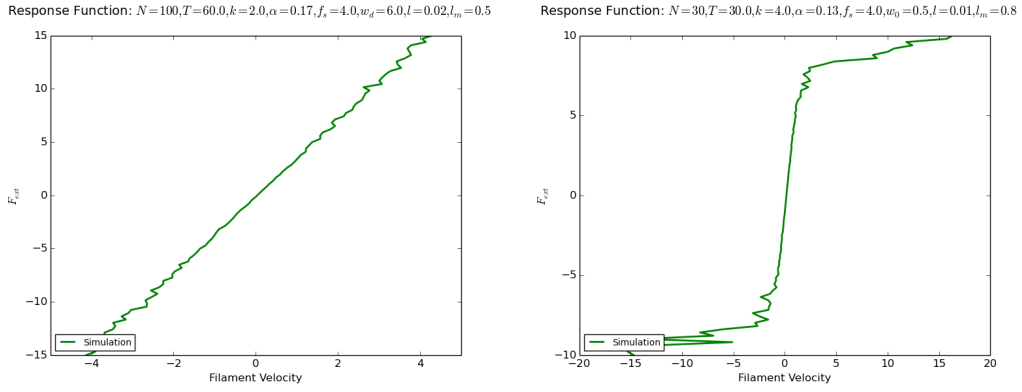

Figure 2.2: (Left) Response diagram of filament velocity vs. external force with a constant detachment rate. (Right) Response diagram with an x-dependent detachment rate.

The simulation with the constant detachment rate, shown in the left image

of Fig. 2.2, shows the expected linear relationship between the external force applied to the filament and its steady-state velocity. There is no hysteresis or sharp transition in this case. The second simulation in Fig. 2.2 with the stretch dependent detachment rate shows a sharp transition and a behaviour that is consistent with hysteresis and bistability. It is very difficult to see the bistability in these simulations explicitly. This is because we are calculating a single steady state velocity per external force while bistability would require two steady-state velocities for a single external force. To find the bistability we must select an external force, where we expect bistability, and do many simulations for this single external force, record the steady-state velocity each time and plot a histogram showing the probability distribution of the steady-state velocity at a certain time. If this probability distribution has a bimodal shape it means we have bistability: two values of the steady-state velocity are highly probable for a single external force. We have done this but could not find bistable velocities. It is in general quite difficult to find bistability hysteresis by direct simulation because one of the stable states may be metastable. To find metastable states we need to study fluctuations, which are in general quite difficult to study as they are by definition rare. We will study a crude model for molecular motors so that we can study the fluctuations analytically.

Our goal is to show how fluctuations and thus possibly bistability, can be studied using large deviation theory. We do this in the context of a simpler version of the model given by Eqs. (2.1.1) and (2.1.2). In the next sections we will study the system described above in a crude approximation where the motors are stiff to study the dominant behaviour of a single motor at long times, the time-dependent, dominant behaviour of many motors and the dominant behaviour of many motors at long times.

2.2 Stiff motor assumption

We consider first a single motor. In Fig. 2.3 we show the same simulation as in Fig. 2.1 but with a large spring constant k_s. The simulation shows that a filament being moved by a single motor with a stiff spring can essentially be described as having two different velocities. The flow field of motor and filament velocity shows that given any initial conditions the system almost instantaneously reaches the steady state. This means there is a very short transient time between the motor attaching and the state where the motor is stretched to apply the stall force f_s. In the single motor case this means that the filament moves with one of two velocities.

Let $\alpha(t)$ be 0 or 1 depending on whether the motor is unattached or attached respectively and let $v(\alpha(t))$ be the velocity of the filament. We denote

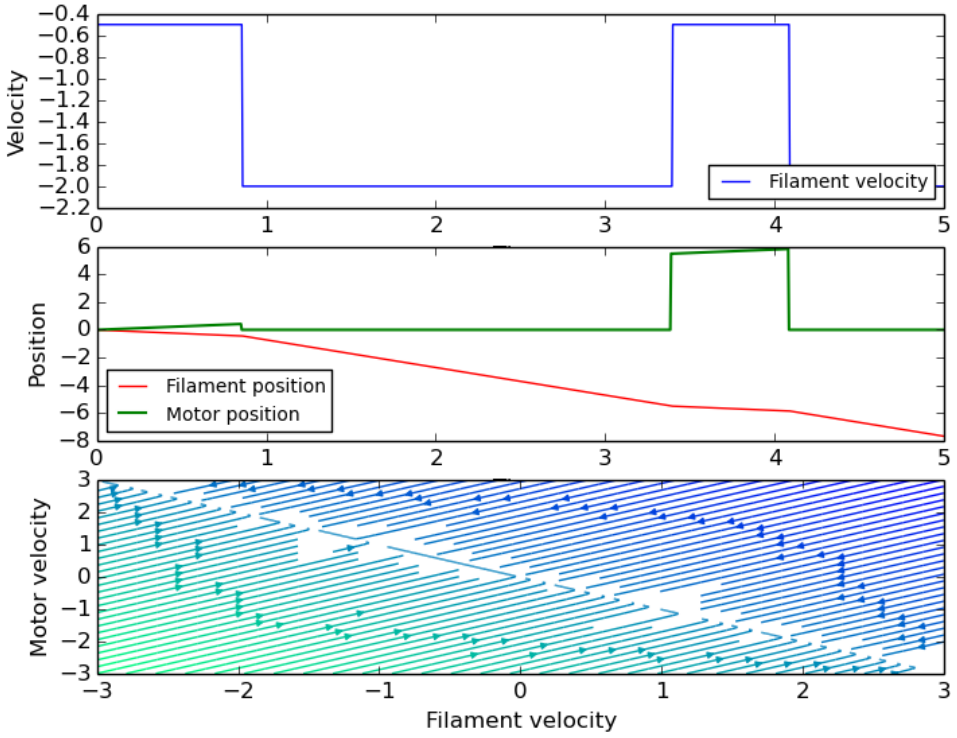

Figure 2.3: A typical process of Eqs. (2.1.1) and (2.1.2) with the stiff-spring approximation. Top - Filament velocity in time, Middle - Motor position along the filament in time, Bottom - Vector field for motor and filament velocity.

each velocity by

$$v(0) = v_0 \tag{2.2.1}$$
$$v(1) = v_1 \tag{2.2.2}$$

such that the position of the filament at time t is given by

$$r(t) = \int_0^t v(\alpha(\tau))\mathrm{d}\tau. \tag{2.2.3}$$

Without the stiff-spring approximation we would need to integrate over the differential equation in Eq. (2.1.2) for the motor evolution and over the attachment and detachment dynamics to get $r(t)$. With this approximation the integral is simply over constant velocities, which switch at random times.

We want to calculate the probability distribution $P(r, t)$ for the position of the filament in time. For this we calculate the generating function of the filament position in time, defined as

$$\begin{aligned}\phi(y,k,t) &= E\left[e^{kr(t)}|\alpha(0)=y\right] \\ &= E\left[\exp(k\int_0^t v(\alpha(\tau))\mathrm{d}\tau)|\alpha(0)=y\right],\end{aligned} \tag{2.2.4}$$

where $k \in \mathbb{R}$.

In the case where $\alpha(t)$ is a Markov process, which is the case when the attachment and detachment rates are constant, the evolution of $\phi(y,k,t)$ is given by the Feynman-Kac equation

$$\frac{\partial\phi(y,k,t)}{\partial t} - (L+kv)\phi(y,k,t) = 0 \tag{2.2.5}$$

with initial condition $\phi(y,k,0)=1$. L is the generator for the Markov process $\alpha(t)$ given by:

$$(L\phi)(y) = \sum_{z\neq y} w(y,z)[\phi(z,k,t)-\phi(y,k,t)] \tag{2.2.6}$$

where $w(y,z)$ is the rate of moving from state y to z. The action of kv is simply

$$(kv\phi)(y) = \sum_z \delta_{zy}\phi(z,k,t)kv(z) = \phi(y,k,t)kv(y). \tag{2.2.7}$$

Since y can take two values, we have two equations with two initial conditions, namely:

$$\begin{aligned}&\frac{\partial\phi(0,k,t)}{\partial t} - w(0,1)[\phi(1,k,t)-\phi(0,k,t)] - kv(0)\phi(0,k,t) = 0 \\ &\phi(0,k,0) = 1\end{aligned} \tag{2.2.8}$$

and

$$\begin{aligned}&\frac{\partial\phi(1,k,t)}{\partial t} - w(1,0)[\phi(0,k,t)-\phi(1,k,t)] - kv(1)\phi(1,k,t) = 0 \\ &\phi(1,k,0) = 1.\end{aligned} \tag{2.2.9}$$

The solutions are plotted in Figs. 2.4, 2.5 and 2.6 for short, intermediate and long times with respect to the equilibration time of the system and the following rates and velocities

$$\begin{aligned}w(0,1) = w(1,0) &= 0.5 \\ v(0) = 1, v(1) &= -1.\end{aligned}$$

This choice of velocities is physically justified, since one can choose the external force to be such that the filament moves at $v(0)=1$ (to the right) when the motor is detached and at $v(0)=-1$ (to the left) when it is attached. The

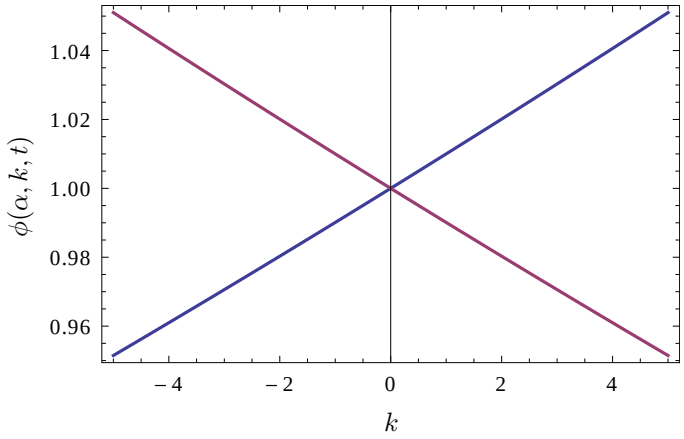

Figure 2.4: $\phi(0, k, t)$ in blue and $\phi(1, k, t)$ in purple (short times).

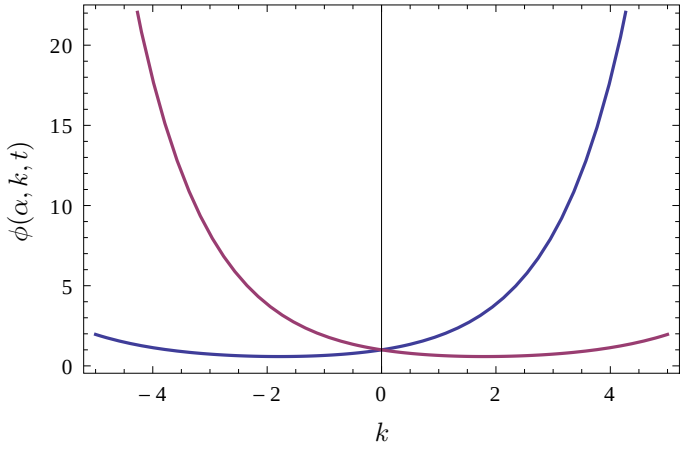

Figure 2.5: $\phi(0, k, t)$ in blue and $\phi(1, k, t)$ in purple (intermediate times).

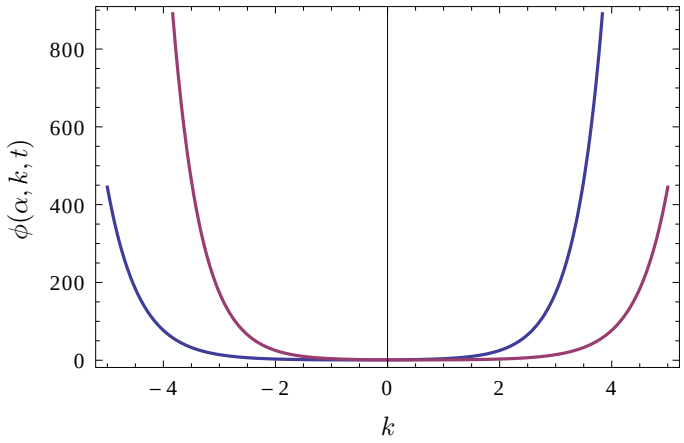

Figure 2.6: $\phi(0, k, t)$ in blue and $\phi(1, k, t)$ in purple (long times).

choice of rates sets the stationary distribution of the motor-state to be in each of the two states with probability $\frac{1}{2}$.

The distribution $P(r,t)$ of the motors position is obtained from these results by taking the inverse Laplace transform. We see from the plots of the two solutions in Fig. 2.4, 2.5 and 2.6 for different times that the graphs change rapidly in time. This makes it difficult to take the inverse Laplace transform exactly. It is however possible to get a qualitative picture of $P(r,t)$ by considering the results at short and long times compared to the equilibration time.

At short times the generating function is a straight line which is the Laplace transform of a delta function. This makes sense since at short times we expect the motor to be close to its initial position with a very high probability. For long times the generating function looks like the Laplace transform of a Gaussian. This means the distribution of the motor position moves from being a delta function at short times to a Gaussian distribution at long times. In the next section we study exactly this long time behaviour of a single motor.

2.3 Long time large deviations for single motor

In this section we describe the system as before, but study $r(t)$ for $t \gg 1$, which is the same as studying the average velocity

$$\bar{v}(t) = \frac{r(t)}{t} = \frac{1}{t}\int_0^t v(\alpha(s))\mathrm{d}s, \tag{2.3.1}$$

where $k \in \mathbb{R}$.

The average velocity becomes constant as $t \to \infty$. We expect fluctuations around this mean value to have a large deviation form, that is

$$P(\bar{v}(t) = v) \approx e^{-tI(v)} \tag{2.3.2}$$

where $I(v)$ is called the rate function and controls the rate of decay of the fluctuations around the mean. The approximation sign $\approx$ here means equality up to sub-exponential fluctuations. The most probable value of the average velocity is given by the zero of the rate function so that the probability of finding the most probable value as $t \to \infty$ becomes 1. An introduction to large deviation theory is given in Appendix A.

As shown in this appendix, we can obtain the rate function $I(v)$ by the Legendre-Fenchel transform of the scaled cumulant generating function (SCGF), $\lambda(k)$. The SCGF is defined as

$$\lambda(k) = \lim_{t\to\infty} \frac{1}{t} \ln\langle e^{tk\bar{v}(t)}\rangle \tag{2.3.3}$$

and the Legendre-Fenchel transform is calculated by

$$I(v) = \sup_k\{kv - \lambda(k)\}. \tag{2.3.4}$$

In the case of a Markov process the SCGF corresponds to the dominant eigenvalue of a transformed generator L_k called the tilted generator, which which for $\bar{v}$ has the form $L_k = L + kv$. Thus we have

$$\lambda(k) = \xi_{max}(L_k) \tag{2.3.5}$$

where $\xi_{max}(L_k)$ denotes the dominant eigenvalue of L_k.

Our goal is now to calculate the rate function for $\bar{v}$ using these results. To determine the dominant eigenvalue of L_k, we have to solve the equation

$$L_k\psi_n(y) = \lambda_n(k)\psi_n(y). \tag{2.3.6}$$

This is easily done by rewriting Eq. (2.2.5) for each value of $y \in \{0, 1\}$, writing this in matrix form, and by finding the eigenvalue of the resulting matrix. The operator L_k in matrix form is

$$L_k = \begin{bmatrix} -w(0,1) + kv(0) & w(0,1) \\ w(1,0) & -w(1,0) + kv(1) \end{bmatrix} \tag{2.3.7}$$

which has two eigenvalues plotted in Fig. 2.7.

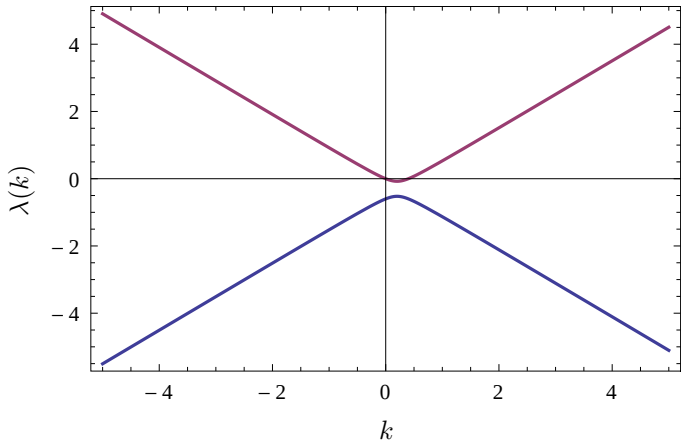

Figure 2.7: Eigenvalues of L_k for $v(0) = 1$, $v(1) = -1$, $w(0,1) = 0.5$ and $w(1,0) = 0.1$.

The SCGF is the largest eigenvalue which, in this case, is the yellow line of Fig. 2.7. To find the rate function we take the Legendre-Fenchel transform as in Eq. (2.3.4) of the SCGF. In this case the SCGF, is differentiable which means we can calculate the transform by taking the derivative of $\lambda(k)$, setting this equal to v to solve for $k = k_v$ and finally plugging this into

$$I(v) = k_v v - \lambda(k_v). \tag{2.3.8}$$

The derivative of $\lambda(k)$ is plotted in Fig. 2.8. Since it has asymptotes at $\lambda'(k) = 1$ and $\lambda'(k) = -1$ the rate function is restricted to be between -1 and

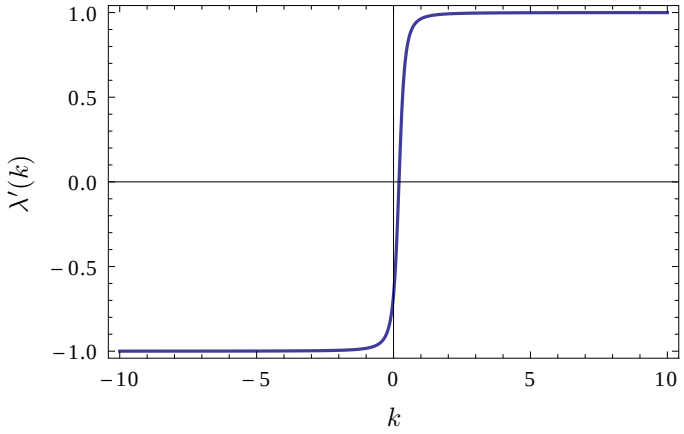

Figure 2.8: $\lambda'(k)$ for $v(0) = 1$, $v(1) = -1$, $w(0,1) = 0.5$ and $w(1,0) = 0.1$.

1. This is because the velocity can only take the values 1 and -1 which means the average velocity has to be between these two values.

The resulting rate function is plotted in Fig. 2.9 for attachment rates larger than the detachment rates so that we expect the filament to be moving with a velocity of -1 most of the time. The average velocity has its most probable value (the zero of the rate function) somewhere between -1 and 0. This is confirmed by Fig. 2.9.

The rate function we find not only gives us the mean velocity but also characterises the probability associated with the fluctuations around this value according to Eq. (2.3.2). It is in this case not symmetric about its zero which means that the fluctuations are not globally Gaussian. The fluctuations close to the zero are Gaussian but as you move further away they become non Gaussian. The rate function shows that it is much less likely to move with velocities to the right of the zero than to the left. This is due to the asymmetry of the rates. The result of this section is precisely the result we announced in Section 2.2.

2.4 Many motors with one filament

In this section we use the same approximation as before but want to calculate the time-dependent rate function for many motors moving on one filament. This is motivated by the fact that bistable behaviour is expected to arise when many motors attach and detach on the same filament.

We are now not considering the velocity of the filament as a result of a motor being attached any more, but the force each motor exerts on the filament when attached $f(\alpha(t) = 1) = f_s$ and the force when not attached $f(\alpha(t) = 0) = 0$. The quantity or random variable (RV) we are interested in is then the average

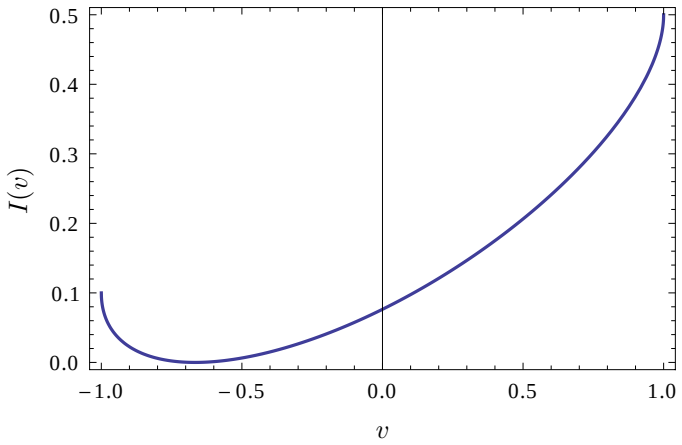

Figure 2.9: Rate function $I(v)$ for $v(0) = 1$, $v(1) = -1$, $w(0,1) = 0.5$ and $w(1,0) = 0.1$.

force exerted per motor in time

$$F_N(t) = \frac{1}{N}\sum_{i=1}^{N} f(\alpha_i(t)) \tag{2.4.1}$$

where the α's are the jump processes for each of the motors determining whether the motor is attached or not. These are taken to be independent but not identically distributed, since the initial state of each motor might be distributed differently. We want to approximate the probability density function for this quantity as before in a large deviation way

$$P(F_N(t) = \bar{f}) \approx \exp\left[-NI(\bar{f}, t)\right]. \tag{2.4.2}$$

To get the rate function using Eq. (2.3.4) we need the generating function of $F_N(t)$

$$E\left[\exp(NkF_N(t))\right] = \prod_i E\left[\exp(kf(\alpha_i(t)))\right], \tag{2.4.3}$$

which can be written as a product due to the independence of the motors. Each of the terms in the product can be calculated by

$$E\left[\exp(kf(\alpha(t)))\right] = \sum_{\alpha=0,1} p(\alpha, t)\exp(kf(\alpha)) \tag{2.4.4}$$

where $p(\alpha, t)$ is the probability of finding a motor in state α at time t.

Since $\alpha(t)$ is a Markov process the evolution of $p(\alpha, t)$ is given by

$$\partial_t p(\alpha, t) = L^\dagger p(\alpha, t) \tag{2.4.5}$$

with initial condition $p(\alpha_0, 0)$ and where $L^\dagger = L^T$. The generator L is as in Eq. (2.2.6), so that Eq. (2.4.5) is explicitly

$$\partial_t p(0,t) = -w_a p(0,t) + w_d p(1,t) \tag{2.4.6}$$

$$\partial_t p(1,t) = w_a p(0,t) - w_d p(1,t) \tag{2.4.7}$$

for the two values of α. The attachment and detachment rates are given here by w_a and w_d respectively. Our evolution operator can be written in matrix form as

$$L^T = \begin{bmatrix} -w_a & w_d \\ w_a & -w_d \end{bmatrix}.$$

This matrix has eigenvalues $\lambda_1 = 0$ and $\lambda_2 = -(w_a + w_d)$ and right eigenvectors $[1, \frac{w_a}{w_d}]^T$ and $[1, -1]^T$, which leads to the solutions

$$p(0,t) = a_1 \exp[-(w_a + w_d)t] + a_2 \tag{2.4.8}$$

$$p(1,t) = -a_1 \exp[-(w_a + w_d)t] + a_2 \frac{w_a}{w_d}. \tag{2.4.9}$$

The constants a_1 and a_2 are given by the initial conditions. We consider next two initial conditions, namely, all motors having the same initial probability distribution and then fixing the number of motors in each state initially (each motors is in one of the states with certainty at $t = 0$).

2.4.1 All motors have the same initial conditions

We will consider two examples for the case where the motors all have the same initial distribution. In the first example we let each motor be in either state with probability $\frac{1}{2}$. Our initial condition for all motors is thus

$$p(0,0) = \frac{1}{2} \tag{2.4.10}$$

$$p(1,0) = \frac{1}{2} \tag{2.4.11}$$

from which we can solve for the constants in Eq. (2.4.8) to obtain

$$a_1 = \frac{\frac{w_a}{w_d} - 1}{2(\frac{w_a}{w_d} + 1)}, \quad a_2 = \frac{1}{1 + \frac{w_a}{w_d}}. \tag{2.4.12}$$

To simplify the calculation, we take the rates to be equal $w_a = w_d = w$. In this case the SCGF is

$$\lambda(k) = \ln\left(\frac{1}{2}e^{kf(0)} + \frac{1}{2}e^{kf(1)}\right). \tag{2.4.13}$$

This can be seen by using the definition of the SCGF as well as Eq. (2.4.4). We have plotted Eq. (2.4.13) in Fig. 2.10.

Notice that this has no time dependence since the initial condition is the steady state distribution. Taking the Legendre-Fenchel transform of the SCGF gives us the rate function

$$I(\bar{f}) = \bar{f} \ln\left[-\frac{\bar{f}+1}{\bar{f}}\right] - \ln\left[\frac{1}{2}\left(-\frac{1+\bar{f}}{\bar{f}}\right)^{-1}\right] \tag{2.4.14}$$

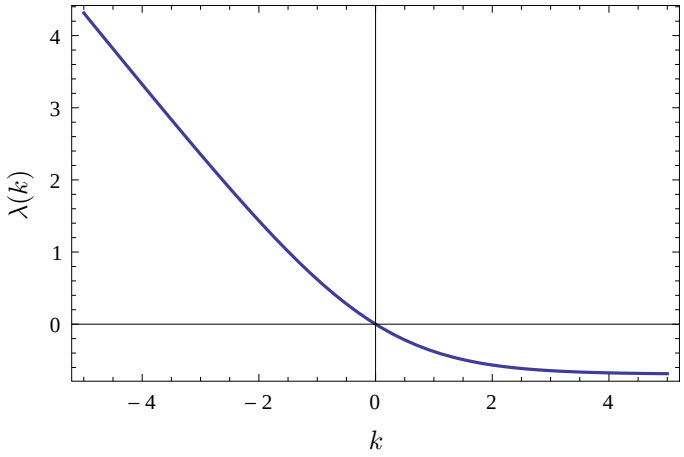

Figure 2.10: The SCGF $\lambda(k)$ for $f(0) = 0$, $f(1) = -1$, $w = 0.1$.

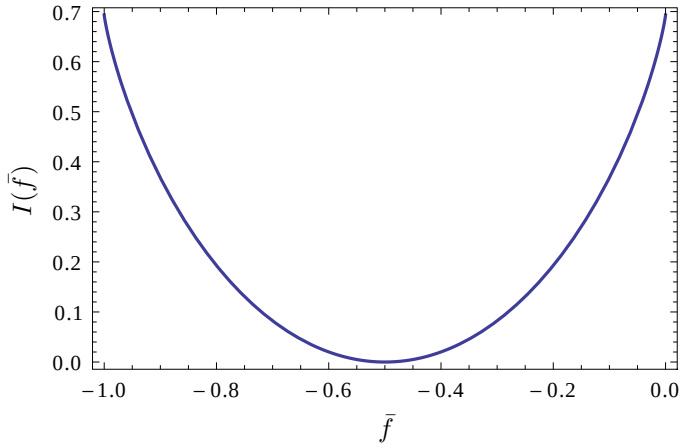

Figure 2.11: Rate function $I(\bar{f})$ for $f(0) = 0$, $f(1) = -1$, $w = 0.1$.

which is plotted in Fig. 2.11. The rate function gives the mean force per motor at -0.5 and the fluctuations around this are Gaussian. The fluctuations near the boundaries -1 and 0 are however non-Gaussian since the rate function is restricted to be between those two values and becomes very steep close to them.

In the second example we take the rates to be equal as before and choose the initial conditions to be

$$p(0,0) = 1 \tag{2.4.15}$$
$$p(1,0) = 0. \tag{2.4.16}$$

In this case all the motors start detached. Following the procedure from before

we find the SCGF

$$\begin{aligned}\lambda(k,t) &= \lim_{N\to\infty}\frac{1}{N}\ln\left[\prod_i E\left[\exp(kf(\alpha_i))\right]\right] \\ &= \ln\left[\frac{1}{2}\exp(-2wt+kf(0))+\frac{1}{2}\exp(kf(0))\right. \\ &\quad \left.-\frac{1}{2}\exp(-2wt+kf(1))+\frac{1}{2}\exp(kf(1))\right] \end{aligned} \tag{2.4.17}$$

and rate function

$$\begin{aligned} I(\bar{f},t) =& f\ln\left(-\frac{(e^{2wt}-1)(1+\bar{f})}{\bar{f}(e^{2wt+1})}\right) \\ &-\ln\left(\frac{1}{2}+\frac{1}{2}e^{-2wt}-\frac{(e^{2wt}+1)\bar{f}}{2(e^{2wt}-1)(1+\bar{f})}+\frac{e^{-2wt}(e^{2wt}+1)\bar{f}}{2(e^{2wt}-1)(1+\bar{f})}\right) \end{aligned} \tag{2.4.18}$$

with $f(0)=0$ and $f(1)=-1$.

We have plotted the rate function for short, intermediate, and long times relative to the equilibration time in Fig. 2.12.

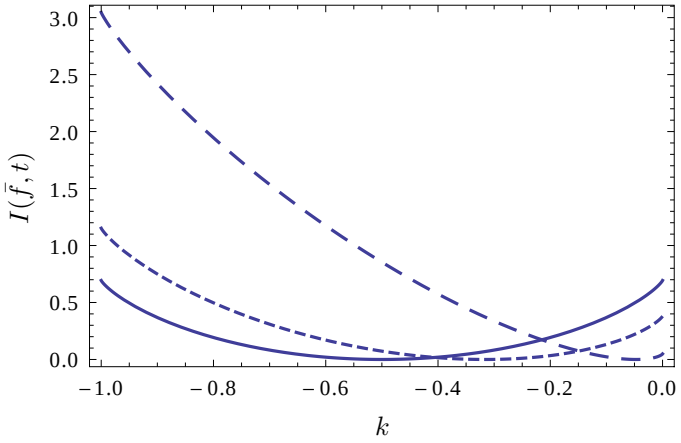

Figure 2.12: $I(\bar{f},t)$ for $f(0)=0$, $f(1)=-1$, $w=0.1$ at different times: short (large dashed), intermediate (small dashed) and long (solid).

This rate function is time dependent. The zero of the rate function at short times is close to zero as expected. It is not symmetric about its zero initially but, as the rate function evolves, the zero moves to -0.5 and the function becomes symmetric. At long times the rate function is the same as the steady-state rate function from the previous example shown in Fig. 2.11. The fluctuations at long times are Gaussian close to the mean but non-Gaussian near the boundaries as before.

2.4.2 Fixing the number of motors in each state initially

In this section we pick N_0 motors to be unattached at time $t = 0$, and N_1 motors to be attached. The SCGF is calculated using the first line of Eq. (2.4.17). In the previous section the expectation was the same for all of the motors, but now we split the product into the product over the expectation value for the motors starting attached and that for the motors starting detached. The SCGF then becomes

$$\lambda(k,t) = \frac{N_0}{N} \ln E_{N_0} + \frac{N_1}{N} \ln E_{N_1} \tag{2.4.19}$$

where

$$E_{N_0} = \frac{1}{2}\left(e^{-2wt+kf(0)} + e^{kf(0)} - e^{-2wt+kf(1)} + e^{kf(1)}\right) \tag{2.4.20}$$

$$E_{N_1} = \frac{1}{2}\left(-e^{-2wt+kf(0)} + e^{kf(0)} + e^{-2wt+kf(1)} + e^{kf(1)}\right) \tag{2.4.21}$$

If we take half of the motors to be unattached and half attached (i.e. $N_0 = N/2$ and $N_1 = N/2$), we find that the resulting rate function is the same as Eq. (2.4.14) in the long time limit. We plot the derivative of the SCGF for this case in Fig. 2.13, which is between -1 and 0 as expected.

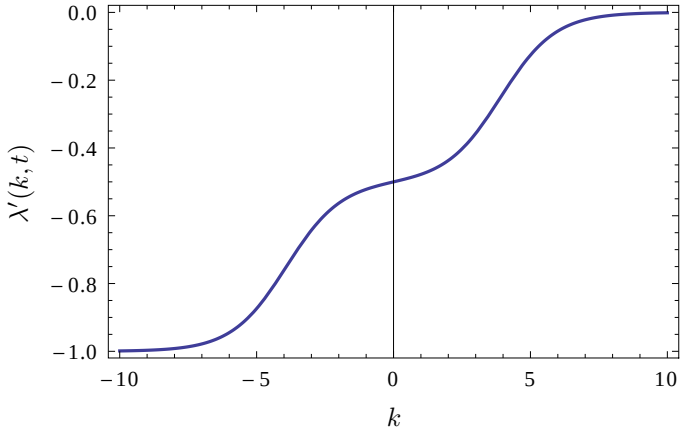

Figure 2.13: $\lambda'(k,t)$ for $f(0) = 0$, $f(1) = -1$, $w = 0.1$.

To compare the rate functions at different times we have plotted in Fig. 2.14 the rate function at short, intermediate, and long times in relation to the time it takes to reach the stationary distribution. This rate function is time dependent because each motor starts with a delta function as initial distribution which means large fluctuations around the most probable value at short times are very improbable. This translates to a steep rate function at short times as seen from the dotted line of Fig. 2.14. As the system evolves the distribution for the state of each motor approaches the steady-state distribution (Eqs. (2.4.10) and (2.4.11)) and large fluctuations in $\bar{f}$ become more probable which is reflected

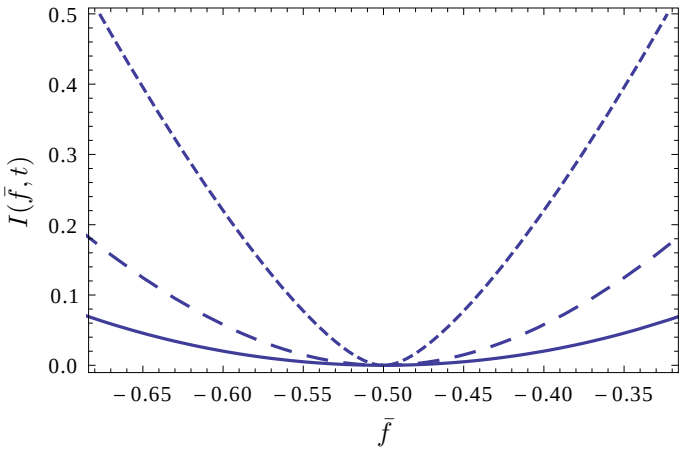

Figure 2.14: $I(\bar{f},t)$ for $f(0)=0$, $f(1)=-1$ and $w=0.1$. dotted - short times, dashed - intermediate times and solid - long times.

in the flattening of the rate function as time progresses. As $t\to\infty$, the rate function converges to the rate function found in Fig. 2.11, as expected.

2.5 Large deviation in time and number of motors

We finish with the behaviour of N motors in the stiff motor limit at long times. The difference from the previous section is that we will study the large deviations as the number $N\to\infty$ in the long-time limit $T\to\infty$. This limit is where we could in principle find bistability since this will give us the steady-state velocity for the many motor case.

Our system is now described by the following equation:

$$\frac{\mu_f}{N}\dot{r}(t)=\frac{1}{N}\sum_i f(\alpha_i(t)) \tag{2.5.1}$$

where i labels the motors and the α's are, as before, the jump processes describing the attachments ($\alpha=1$) and detachments ($\alpha=0$) of the motors. We want to approximate the probability density of the average force per motor at long times, which is given by

$$\bar{F}_{T,N}=\frac{1}{NT}\int_0^T\sum_{i=1}^N f(\alpha_i(t))\mathrm{d}t. \tag{2.5.2}$$

As before we expect the probability density to have a large deviation form but now in the double limit $N\to\infty$ and $T\to\infty$, so that

$$P(\bar{F}_{T,N}=\bar{f})\approx\exp\left[-NTI(\bar{f})\right]. \tag{2.5.3}$$

The generator L of all of the jump processes is the direct sum of the operators of the individual jump processes, and each motor switches between the same two forces. We can represent our operator by a matrix as follows

$$L = \begin{bmatrix} L_1 & 0 & 0 & \dots & 0 \\ 0 & L_2 & 0 & \dots & 0 \\ 0 & 0 & L_3 & \dots & 0 \\ \vdots & \vdots & \vdots & \ddots & \vdots \\ 0 & 0 & 0 & \dots & L_N \end{bmatrix}$$

Since each motor can switch between the same two forces, the total tilted generator is the sum

$$L_k = \sum_i L_{i,k} \tag{2.5.4}$$

where $L_{i,k}$ is the tilted generator of the i^{th} motor. We need to calculate the dominant eigenvalue of the this $2N \times 2N$ matrix by solving the equation

$$\det(L_k - \lambda I_{2N}) = 0. \tag{2.5.5}$$

This can be simplified, since this is a block diagonal matrix, to

$$\det(L_1 - \lambda I_2) \times \det(L_2 - \lambda I_2) \times \dots \times \det(L_N - \lambda I_2) = 0. \tag{2.5.6}$$

Since all the sub-matrices are the same, the dominant eigenvalue is just the dominant eigenvalue of one of the sub-matrices. This gives us the same rate function previously plotted in Fig. 2.9. The result is as we expect since the motors here are independent and do not interact. The difference here is that the approximated probability density function is given by Eq. (2.5.3).

The probabilities associated with fluctuations around the most probable value in equation (2.5.3) exponentially decrease as a function of both T and N. This means finding a value for the average force per motor in time other than the zero of the rate function for a system of many motors is highly improbable.

2.6 Conclusion

In this chapter we have used a very crude approximation, where we take the motors to be stiff, to study the mean force exerted by molecular motors and the fluctuations around it using large deviation theory. The motion of molecular motors involves two stochastic processes. The first process switches the motor between the two states, namely; attached and detached. We take this switching to be a Markov process, but this could be reformulated to include non-Markovian switching dynamics. The second is the biased diffusion the

motor performs along the filament, which becomes deterministic in the stiff motor approximation.

We calculate the large deviation rate function for the mean filament velocity and mean motor force and study how the rate function depends on the initial distribution of molecular motors. The rate function gives us information about the most probable value for the mean filament velocity and mean motor force but goes beyond mean-field calculations because it also characterises the fluctuations around it.

The bistability found in [9] does not show up in the stiff motor approximation. This makes sense since the bistability seems to be associated with the stretch dependent detachment rate. Here we took the motor to become fully stretched instantly when attaching so that a stretch dependent rate would again be constant. To find bistability in this approximation we could take the detachment rate to depend on the time the motor has spent being attached to the filament. The alternative is to look at a model that includes the transient part of the motors motion along the filament. In this case it will be possible to include a stretch dependent detachment rate. This model will be the topic of the next chapter.

Chapter 3

Stochastic resetting

In many models the molecular motors are assumed to detach and reattach at zero stretch almost instantaneously. This is a sensible assumption because the time scale of the relaxation and reattachment of the motor is small in comparison with the time the motor spends attached to the filament. When attached, a molecular motor essentially performs a continuous time random walk with linear friction which corresponds mathematically to the Ornstein-Uhlenbeck process.

The instantaneous relaxation of molecular motors can be modelled using resetting of stochastic processes as introduced in Sec. 1.3. Our goal in this chapter is to study the average force a single molecular motor exerts on a filament, as in the previous chapter, when we include the actual dynamics of the motor given by Eq. (2.1.2) with resetting and noise.

Recent papers on stochastic resetting study optimal resetting for diffusions [31], resetting in arbitrary dimensions [32], optimal search times for Lévy-flights with resetting [10] and temporal relaxation in simple diffusion with resetting [33].

3.1 Model

We model the motion of the molecular motor along the filament using a stochastic differential equation with general form

$$\mathrm{d}X_t = F(X_t)\mathrm{d}t + \sigma \mathrm{d}W_t. \tag{3.1.1}$$

Here X_t is the observable of the process, $F(X_t)$ is a general function defining the drift of the process, σ is the strength of the noise and W_t is the Brownian motion. In the case of pure Brownian motion the drift is $F(X_t) = 0$.

In addition to this diffusion we have a sort of jump process that brings X_t back to a constant position x_0 with a probability per unit time r. This is called stochastic resetting and has been studied recently in the context of

search algorithms in computer science [34]. A discrete version of stochastic resetting is studied in catastrophes of birth and death processes [22; 23; 24].

Introducing resetting to a stochastic process changes the evolution of X_t and of its probability density $p(x,t)$. Without reset the evolution of this density is given by the Fokker-Planck equation

$$\partial_t p(x,t) = L^\dagger p(x,t) \tag{3.1.2}$$

where

$$L^\dagger = -\frac{\partial}{\partial x}F(x) + \frac{\sigma^2}{2}\frac{\partial^2}{\partial x^2} \tag{3.1.3}$$

is the dual of the generator L considered before in the context of the Feynman-Kac equation.

When including reset the modified Fokker-Planck equation is

$$\partial_t p(x,t) = (L^\dagger - r)p(x,t) + r\delta(x - x_0). \tag{3.1.4}$$

This makes sense as resetting should subtract probability at a rate r from all points due to the possibility of a reset at any time. Since resetting sets $x = x_0$ the probability subtracted from all other points is placed at the resetting position x_0. The derivation of this modification is in Appendix B.

It is shown in [34] that $p(x,t)$ can be obtained using a renewal argument to find an equation relating the solution of the process with reset to the one without reset. They argue that the probability of finding $X_t = x$ at time t for the process with reset is the same as the probability of finding $X_\tau = x$ at time τ for the pure diffusion where τ is the amount of time t that has passed since the last reset. This is because X_t just undergoes normal diffusion from the last reset till the time of observation.

To be more specific the particle either reaches time t without being reset with probability e^{-rt} or it is reset last at time $t-\tau$ and undergoes pure diffusion till time t with probability $re^{-r\tau}$. To find the reset solution we must add these two contributions and integrate over all possible last reset times. If we take $p_0(x,t)$ as the solution for no drift diffusion without reset, we can then write

$$p(x,t) = p_0(x,t)e^{-rt} + \int_0^t re^{-r\tau}p_0(x,\tau)\mathrm{d}\tau. \tag{3.1.5}$$

The easiest way to see the equivalence of this equation and Eq. (3.1.4) is by taking the Laplace transform of both equations and then checking the consistency of the two equations by plugging one in the other. We recall that the Laplace transform of a function $f(t)$ is given by

$$\mathcal{L}[f(t)] = \tilde{f}(s) = \int_0^\infty e^{-ts}f(t)\mathrm{d}t \tag{3.1.6}$$

Taking the Laplace transform of Eqs. (3.1.4) and (3.1.5) gives

$$s\tilde{p}(x,s) - p(x,0) = (L - r)\tilde{p}(x,s) + \frac{r}{s}\delta(x - x_0) \tag{3.1.7}$$

and

$$\tilde{p}(x,s) = \frac{r+s}{s}\tilde{p}_0(x,s). \tag{3.1.8}$$

Plugging Eq. (3.1.8) into Eq. (3.1.7) and using the fact that

$$\partial_t p_0(x,t) = Lp_0(x,t) \tag{3.1.9}$$

we find

$$-s\delta(x-x_o) = -s\delta(x-x_o) \tag{3.1.10}$$

proving the equivalence. This renewal argument was used in [34] to derive a stationary distribution for the probability density function.

3.2 Additive observables with reset

In this section we study the same model but instead of studying the probability density function of X_t we are interested in studying the fluctuations of integrals of functions of X_t. In other words we will study additive observables having the form

$$A_T = \frac{1}{T}\int_0^T f(X_t)\mathrm{d}t \tag{3.2.1}$$

where f is now an unspecified function of X_t.

Previous studies on stochastic resetting have not studied additive observables and our goal in this chapter is to generalise the renewal argument from before to include additive observable and to use large deviation theory with the generalised renewal argument to study the fluctuations of additive observables in the context of molecular motors. Our renewal argument will find a relation of the same type between the two generating functions of an additive observable with and without reset.

To study the fluctuations of additive processes we approximate the probability density function using the rate function as we did in the previous chapter:

$$P(A_T = a) \approx e^{-TI(a)}. \tag{3.2.2}$$

The evolution of the generating function for this observable is governed by the Feynman-Kac evolution equation as seen in Chap. 2. We will now derive the Feynman-Kac evolution equation for the generating function of A_T with reset, defined as

$$G_r(x,k,T) = E_x[e^{TkA_T}] = E\left[e^{k\int_0^T f(X_s)\mathrm{d}s}|X_0 = x\right] \tag{3.2.3}$$

where x is the initial position and $E[\cdot]$ is the usual expectation value with respect to the process with reset. To derive an evolution equation for $G_r(x,k,T)$

we start by writing for the process without resetting

$$G_0(x,k,T+\mathrm{d}T) = e^{kf(x)\mathrm{d}T}\int \mathrm{d}x' p(x') E^0_{x'}[e^{k\int_{\mathrm{d}T}^{T+\mathrm{d}T} f(X_t)\mathrm{d}t}] \tag{3.2.4}$$

$$= e^{kf(x)\mathrm{d}T}\int \mathrm{d}\zeta K(\zeta) G_0(x+\zeta,k,T) \tag{3.2.5}$$

where in the first step we have removed the first infinitesimal term from the integral in Eq. (3.2.1) and $E^0[\cdot]$ is the expectation value for the process without reset. In the second step we have performed a change of coordinates with ζ being the step size from x to x'. $K(\zeta)$ is the propagator for a step of size ζ and the last step is possible due to the invariance of the process under a shift in time. If one includes reset this is split further into a part where the particle has reset after a time $\mathrm{d}T$ with probability $r\mathrm{d}T$ and one where it has not reset with probability $(1-r\mathrm{d}T)$, so that

$$G_r(x,k,T+\mathrm{d}T) = e^{kf(x)\mathrm{d}T}\left[r\mathrm{d}T G_r(x_0,k,T) + (1-r\mathrm{d}T)\int \mathrm{d}\zeta K(\zeta) G_r(x+\zeta,k,T)\right]. \tag{3.2.6}$$

Taylor expanding the exponential and taking the limit of

$$\frac{G_r(x,k,T+\mathrm{d}T) - G_r(x,k,T)}{\mathrm{d}T} \tag{3.2.7}$$

as $\mathrm{d}T \to 0$ we then find

$$\partial_T G_r(x,k,T) = (L-r)G_r(x,k,T) + rG_r(x_0,k,T) \tag{3.2.8}$$

where L is the mathematical generator of the process corresponding to the adjoint of the operator from Eq. (3.1.3). This is the modified Feynman-Kac evolution equation for the generating function with reset.

We will now use a renewal argument for the generating functions to find a formula which is equivalent to Eq. (3.1.5). We start by noting that the additive observable can be split up into the sum over the times where the particle undergoes diffusion without reset

$$TA_T = \sum_{i=1}^{n+1}\int_{\sum_{j=1}^{i}\tau_{j-1}}^{\tau_i} f(X_s)\mathrm{d}s. \tag{3.2.9}$$

The number of resets is n and the duration of the i^{th} reset is given by τ_i and $\tau_0 = 0$. This gives the condition $T = \sum_{i=1}^{n+1}\tau_i$. The probability of having a reset after time τ is $re^{-r\tau}$ and the probability of no reset till time T is e^{-rT}. The definition of the generating function without reset is

$$G_0(x,k,T) = E^0_x[e^{TkA_T}] \tag{3.2.10}$$

where the 0 indicates again that this is the generating function for the stochastic process without reset and a r would indicate the one with reset.

To find a relation between these two we note that we can split up the generating function into parts where the particle is just undergoing diffusion between resets. This can be done when the number of resets in the time interval T is known. To write the full generating function we then have to sum over the number of resets possible n and integrate over all possible reset times for each term in the sum. This gives

$$G_r(x,k,T) = \sum_{n=0}^{\infty} \int_0^T \mathrm{d}\tau_1 r e^{-r\tau_1} G_0(x,k,\tau_1) \int_0^T \mathrm{d}\tau_2 r e^{-r\tau_2} G_0(x_0,k,\tau_2) \\ \dots \int_0^T \mathrm{d}\tau_{n+1} e^{-r\tau_{n+1}} G_0(x_0,k,\tau_{n+1}) \delta(T - \sum_{i=1}^{n+1} \tau_i). \tag{3.2.11}$$

We note that the generating function for the first reset time has an initial position at x while all others have as initial position the reset position x_0.

It is natural at this point to take the Laplace transform of Eq. (3.2.11) to deal with the delta constraint. The Laplace transform of the delta function is

$$\mathcal{L}\left[\delta(T - \sum_{i=1}^{n+1} \tau_i)\right] = e^{-s\sum_{i=1}^{n+1}\tau_i}. \tag{3.2.12}$$

We start with the $n = 0$ term of the sum which just gives

$$\tilde{G}_0(x,k,s+r). \tag{3.2.13}$$

where the tilde indicates the Laplace transform. When $n = 1$ we find that we are taking the Laplace transform of a convolution giving

$$r\tilde{G}_0(x,k,s+r)\tilde{G}_0(x_0,k,s+r). \tag{3.2.14}$$

The next term gives the convolution of three functions and this continues for higher order terms resulting in a geometric series. Under the condition

$$r\tilde{G}_0(x_0,k,s+r) < 1 \tag{3.2.15}$$

we obtain

$$\tilde{G}_r(x,k,s) = \frac{\tilde{G}_0(x,k,s+r)}{1 - r\tilde{G}_0(x_0,k,s+r)}. \tag{3.2.16}$$

It is simple to prove that this is equivalent to the Feynman-Kac evolution equation given by Eq. (3.2.8) for the generating function using the same procedure as for proving the equivalence of Eqs. (3.1.4) and (3.1.5).

This is the main result of this chapter, which we will use in the following section in a model for molecular motors. The result is fairly general as it hold for any choice of the function $f(X_T)$ in Eq. (3.2.1).

3.3 Ornstein-Uhlenbeck process

In this section we will use the results from before to study a simple linear SDE known as the Ornstein-Uhlenbeck process, in which reset is included. This model is actually equivalent to our original model Eq. (2.1.2) of molecular motors, as argued below, but now with the reset explicitly included. For this model we study the average motor stretch using large deviation theory.

3.3.1 Model

The SDE describing the Ornstein-Uhlenbeck process is

$$\mathrm{d}X_t = -\gamma X_t \mathrm{d}t + \sigma \mathrm{d}W_t \tag{3.3.1}$$

where γ is the friction coefficient, σ is the strength or variance of the noise and $\mathrm{d}W_t$ is the Wiener process.

The additive observable that we study is

$$A_T = \frac{1}{T}\int_0^T X_t \mathrm{d}t \tag{3.3.2}$$

which gives the average motor stretch in time when X_t is evolving according to Eq. (3.3.1). In the context of Eq. (2.1.2), X_t is the same as $r + s$. The Ornstein-Uhlenbeck process is diffusion with linear friction which is essentially the same as Eq. (2.1.2) with the external force $F_{\text{ext}} = 0$. Eq. (3.3.2) is an important observable because it tells us the average force a motor will exert on a filament in time, which in turn tells us with what velocity the filament will move.

This additive observable has already been studied using large deviation theory for the Ornstein-Uhlenbeck process without resetting. Its rate function can be found by symmetrization, as described in Appendix C. The rate function then gives the following approximation of the probability density function:

$$P_0(A_T = a) \approx e^{-TI_0(a)} \tag{3.3.3}$$

and in this case the rate function is

$$I_0(a) = \frac{\gamma^2 a^2}{2\sigma^2}. \tag{3.3.4}$$

For what comes below, it is important to note that, when the random variable obeys a large deviation principle we can approximate the generating function as

$$G_0(x, k, T) \approx g(x)e^{T\lambda_0(k)} \tag{3.3.5}$$

where $\lambda_0(k)$ is the Legendre-Fenchel transform Eq. (2.3.4) of the rate function $I_0(a)$. At the same time $\lambda_0(k)$ is also the largest eigenvalue of the tilted

generator of the process and $g(x)$ is the corresponding eigenfunction. This approximation can be made more accurate by including the next to dominant eigenvalue. If we take the Laplace transform of the approximated generating function Eq. (3.3.5) we get

$$\tilde{G}_0(x,k,s) \approx \frac{g(x)}{s-\lambda_0(k)}. \tag{3.3.6}$$

3.3.2 Results with resetting

We will use Eq. (3.2.16) to calculate the large deviation rate function of the Ornstein-Uhlenbeck process with resetting. We start by decomposing the generating function $G_0(x,s,k)$ for the process without reset over the eigenbasis of its tilted generator, which is

$$L_k = -\gamma x\frac{d}{dx} + \frac{\sigma^2}{2}\frac{d^2}{dx^2} + kx. \tag{3.3.7}$$

Then we calculate its Laplace transform and insert this into Eq. (3.2.16) to find the Laplace transform of the generating function of the process with reset, $\tilde{G}_r(x,s,k)$. The inverse Laplace transform of $\tilde{G}_r(x,s,k)$ will be dominated at long times by its largest pole in s. The dominant pole of $\tilde{G}_r(x,s,k)$ will be the SCGF from which we can calculate the rate function by Legendre-Fenchel transform Eq. (2.3.4).

The right and left eigenfunctions of Eq. (3.3.7) are known to be, respectively,

$$r_{k,i}(x) = A_{r,i}H_i\left(\frac{\sqrt{\gamma}x}{\sigma} - \frac{k\sigma}{\gamma^{3/2}}\right)\exp\left[\frac{kx}{\gamma} - \frac{3k^2\sigma^2}{4\gamma^3}\right] \tag{3.3.8}$$

$$l_{k,i}(x) = A_{l,i}H_i\left(\frac{\sqrt{\gamma}x}{\sigma} - \frac{k\sigma}{\gamma^{3/2}}\right)\exp\left[-\frac{(-2\gamma^2x + k\sigma^2)^2}{4\gamma^3\sigma^2}\right] \tag{3.3.9}$$

where $H_i(x)$ is the i^{th} Hermite polynomial and $A_{r,i}$ and $A_{l,i}$ are constants. The Hermite polynomials can be found recursively by

$$H_{i+1}(x) = 2xH_i(x) - 2iH_{i-1}(x) \tag{3.3.10}$$

with $H_0(x) = 1$ and $H_1(x) = 2x$. The eigenvalues of Eq. (3.3.7) are

$$\lambda_i(k) = \frac{k^2\sigma^2}{2\gamma^2} - i\gamma. \tag{3.3.11}$$

The normalization conditions for the eigenfunctions are

$$1 = \int_{-\infty}^{\infty} l_{k,i}(x)\mathrm{d}x \tag{3.3.12}$$

$$\delta_{i,j} = \int_{-\infty}^{\infty} r_{k,i}(x)l_{k,j}(x)\mathrm{d}x \tag{3.3.13}$$

so that the normalization constants are

$$A_{r,i} = \frac{(-1)^i \gamma^{-\frac{3i}{2}} k^i \sigma^i}{\sqrt{2^n n!}\sqrt{(2n)!!}} \tag{3.3.14}$$

$$A_{l,i} = \frac{(-1)^i \gamma^{\frac{1}{2}+\frac{3i}{2}}}{k^i \sigma^{i+1}} \frac{\sqrt{(2i)!!}}{\sqrt{2^i \pi i!}}. \tag{3.3.15}$$

With these results, we can write an exact expression for $G_0(x, k, T)$

$$G_0(x, k, T) = \sum_{i=0}^{\infty} r_{k,i}(x) e^{T\lambda_i(k)}, \tag{3.3.16}$$

where we have absorbed the expansion coefficients in the eigenfunctions.

The Laplace transform of Eq. (3.3.16) is then

$$\tilde{G}_0(x, k, s) = \sum_{i=0}^{\infty} \frac{r_{k,i}(x)}{s - \lambda_i(k)}. \tag{3.3.17}$$

The largest pole of this equation that determines the SCGF because it will dominate the sum in Eq. (3.3.16) when T is large. To locate this pole numerically, we truncate the sum in Eq. (3.3.17) at some order m when we insert it in Eq. (3.2.16). We start by truncating at $m = 1$, which is a good approximation at long times since this includes the dominant eigenvalue.

From the properties of the SCGF we know that it must be convex and that $\lambda_r(0) = 0$. The largest pole of Eq. (3.3.17) when using the $m = 1$ truncated sum in Eq. (3.2.16) is non-convex. This means that it cannot be the SCGF for the Ornstein-Uhlenbeck process with reset. If we include the next to dominant term in Eq. (3.3.17) we find that the non-convexity is less pronounced. Including higher and higher modes in Eq. (3.3.17) eventually produces a convex largest pole and it is this pole that we take as the SCGF. This convergence to a convex largest pole when including higher modes is illustrated nicely by taking $x_0 = 0$, $\gamma = 1$, $\sigma = 1$, $r = 2$ and calculating the largest pole for different number of modes which can be seen in Fig. 3.1. Only including the lowest mode produces the blue line and as one includes more modes the largest pole approaches the convex green line.

To study the convergence of the SCGF with m, we plot the difference between consecutive poles for the case where the reset position is zero and then for the case where it is non-zero. We expect the convergence to take longer in the non-zero reset case. We use the mode truncation after which the difference between the previous and current largest pole is $\epsilon = 0.01$ and find that for both zero and non-zero x_0 this value is reached when including the 9^{th} mode. In Fig. 3.2 we plot

$$\delta\lambda_r^m = \int_{-\infty}^{\infty} |\lambda_r^{m+1}(k) - \lambda_r^m(k)| \mathrm{d}k \tag{3.3.18}$$

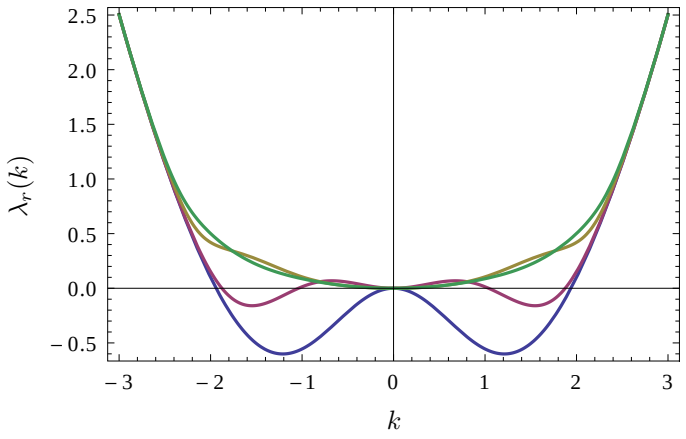

Figure 3.1: Largest poles, $\lambda_r(k)$, of $\tilde{G}_r(x, s, k)$ for different mode truncations with $x_0 = 0$ and $r = 2$. The first is $m = 1$ in blue and the last is $m = 5$ in green.

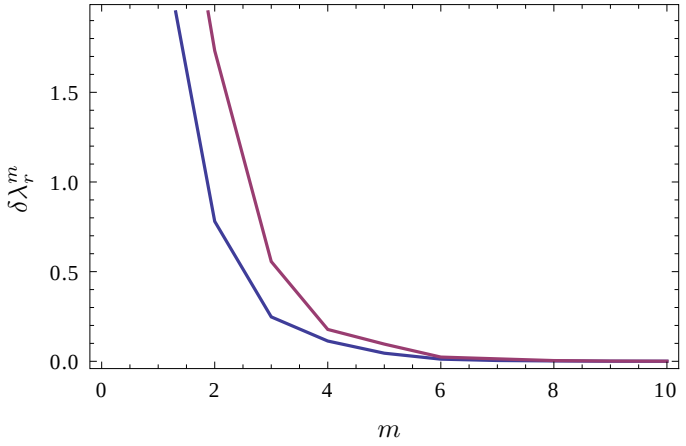

Figure 3.2: Difference between consecutive SCGF against number of modes included for $r = 2.0$ and $x_0 = 0.0$ (blue) $x_0 = 1.0$ (purple).

as a function of m. We plot both the convergence for a zero reset position $x_0 = 0$ and a non-zero reset position $x_0 = 1.0$ with $r = 1$. There seems to be only a slight difference in the speed of the convergence when the reset position is shifted to $x_0 = 1.0$.

This procedure of including higher modes to get rid of non-convexity is in theory possible for any resetting rate r but becomes computationally expensive above $r = 3$.

The reason for the non-convexity in the largest pole when only one mode is included in the eigenvalue expansion of the generating function is due to the Ornstein-Uhlenbeck process with reset being made up of many parts that undergo the Ornstein-Uhlenbeck process without reset for a finite time and therefore require in principle the exact expression of the generating function.

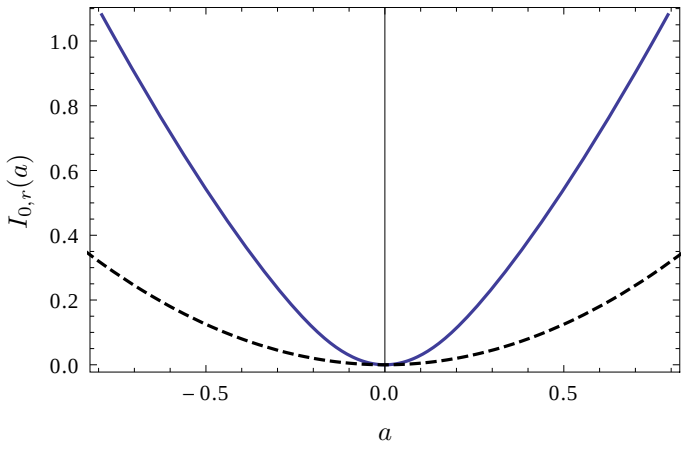

Figure 3.3: Comparison of $I_0(a)$ (dashed) and $I_r(a)$ (solid) with $x_0 = 0.0$ and $r = 2$.

The approximation with only the dominant eigenvalue is exact in the long time limit, but when the process keeps restarting this is never reached. The approximation then needs to be accurate for the typical time of renewal part of the process. This depends on the resetting rate r. If the rate is small there are not that many resets meaning a less exact generating function will be a sufficient approximation, which translates into including a smaller number of modes. As the resetting rate is increased more resets take place in the same amount of time and more modes are needed to make the generating function for each part more exact.

We cannot calculate the Legendre-Fenchel transform of the SCGF numerically but can plot it as

$$(\lambda_r'(k); k\lambda_r'(k) - \lambda_r(k)). \tag{3.3.19}$$

The result is shown with the original rate function ($r = 0$) in Fig. 3.3. The rate function with reset behaves as expected. It is steeper than the rate function without reset showing that it is more probable to find the particle closer to the reset position than in the no reset case. It is also symmetric around the zero and the fluctuations close to zero are Gaussian. This is because the rate function with $r = 0$ is Gaussian and from the plot we see that the two functions are the same close to zero.

We now investigate how this the rate function is changed when we take a non zero reset position. In Fig. 3.4 we have plotted the largest pole when including different number of modes where the reset position is $x = 0.5$. We see that it converges to a SCGF that has its minimum shifted to the left. We expect the corresponding rate functions minimum a^* to shift away from the origin in the direction of the reset position which in this case is to the right. If the resetting rate is strong enough the concentration point should again be on the resetting position.

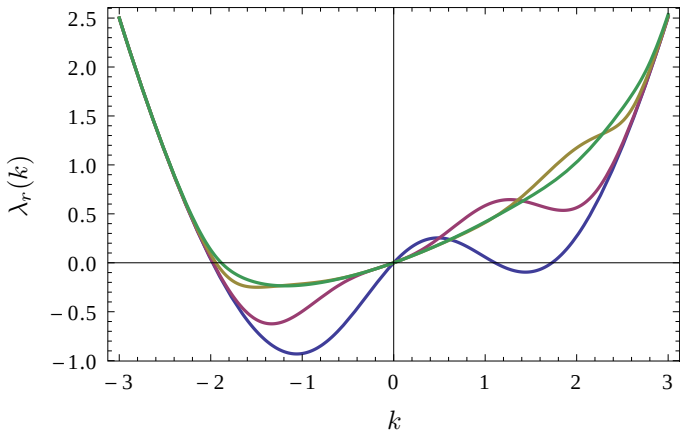

Figure 3.4: Largest poles, $\lambda_r(k)$, of $\tilde{G}_r(x, s, k)$ for different mode truncations with $x_0 = 0$ and $r = 2$. The first is $m = 1$ in blue and the last is $m = 5$ in green.

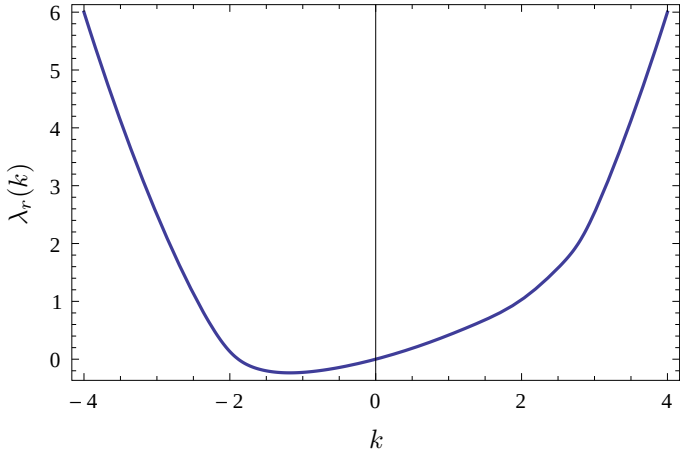

Figure 3.5: SCGF with $x_0 = 0.5$ and $r = 2$.

We cannot take r very large since in this case we need to include a high number m of modes to get an accurate rate function and this is computationally out of reach. We take $r = 2$ as this demonstrates the effect well. The SCGF for the process with the reset position moved to $x_0 = 0.5$ is plotted in Fig. 3.5 and the corresponding rate function is plotted in Fig. 3.6. The rate function is clearly shifted in the direction of the new reset position and is again steeper than the rate function without reset. It is still symmetric around its zero.

The minimum of the rate function gives the point of concentration in the long time limit where, according to the large deviation principle

$$P(A_T = a) \approx e^{-TI_r(s)} \tag{3.3.20}$$

as $T \to \infty$. We therefore study how this minimum changes when varying either the reset position or the reset rate while keeping the other constant. In

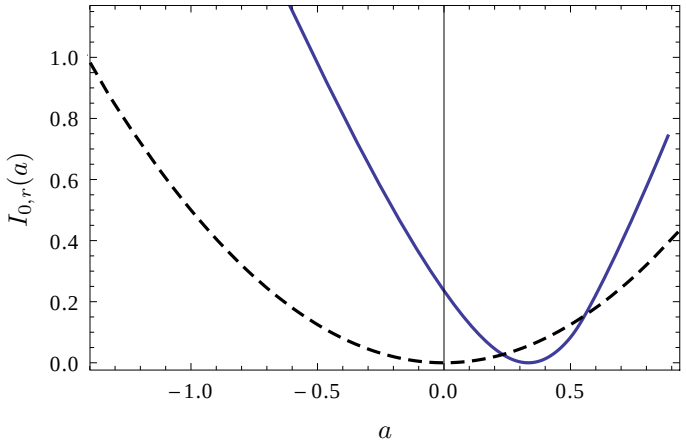

Figure 3.6: Comparison of $I_0(a)$ (dashed) and $I_r(a)$ (solid) with $x_0 = 0.5$ and $r = 2$.

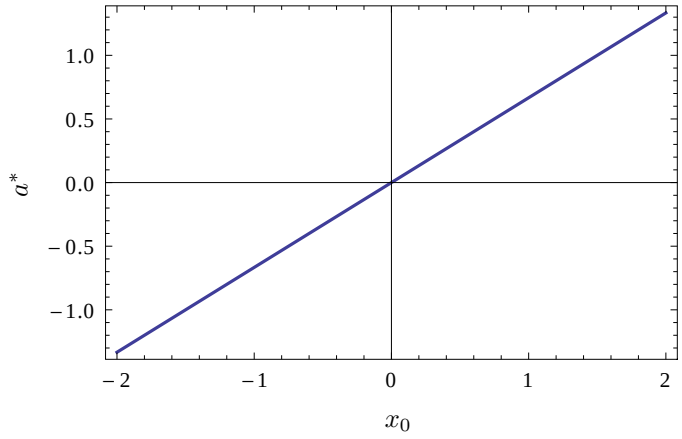

Figure 3.7: Position of the minimum a^* of the rate function $I_r(a)$ versus resetting position x_0 with $r = 2$.

Fig. 3.7 we have kept the resetting rate constant and varied the reset position. This results is linear which makes sense since the strength of the resetting is the same and we are only shifting the position it is resetting to. In Fig. 3.8 we have done the the same but now keeping the reset position at $x_0 = 0.5$ while varying the resetting rate r. The function plotted in Fig. 3.8 has an asymptote at $a^* = 0.5$. We see that increasing r moves the minimum closer and closer to the reset position and in the limit as $r \to \infty$ the minimum will be at $x_0 = 0.5$.

Finally we have written a computer simulation using the Euler method of the Ornstein-Uhlenbeck process with resetting using an Euler method to test our results. In Fig. 3.9 we have compared the simulation at different times with the analytic results in the case where $x_0 = 0$ and in Fig. 3.10 we have done the same with $x_0 = 0.5$. The simulations match the analytic

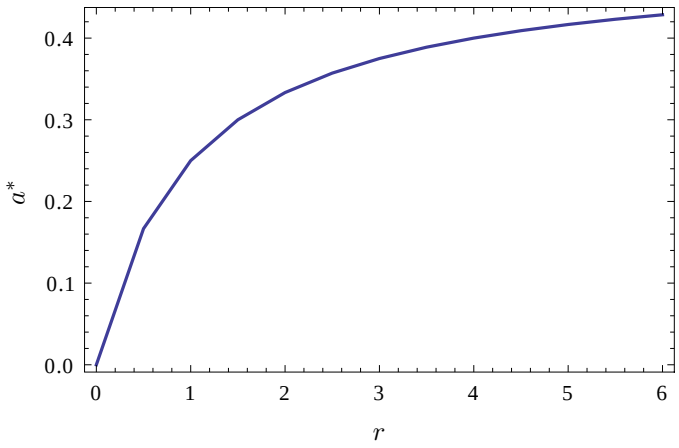

Figure 3.8: Position of the minimum a^* of the rate function $I_r(a)$ versus resetting rate r with $x = 0.5$.

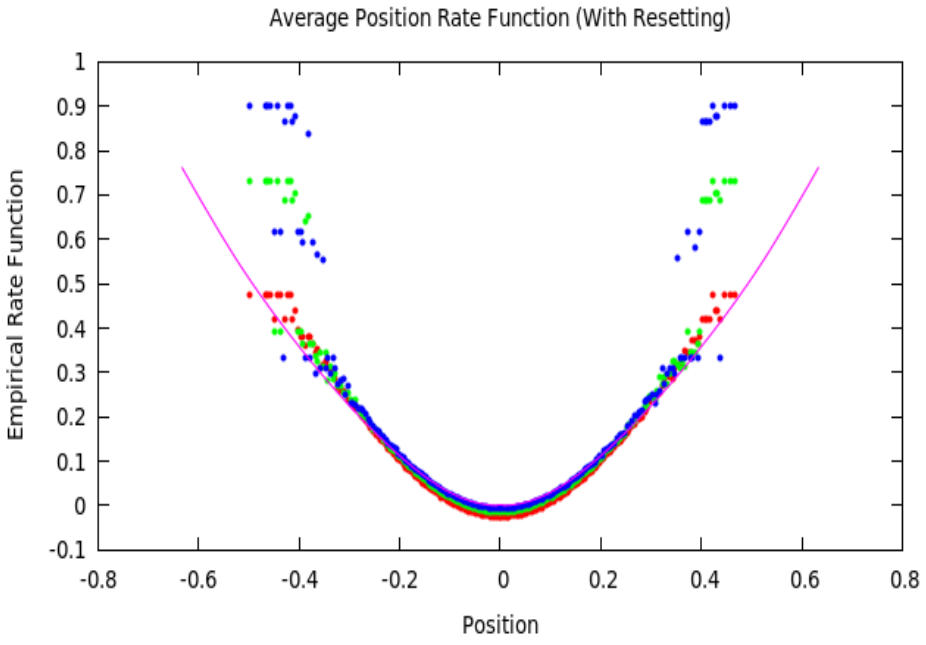

Figure 3.9: Comparison of $I_r(a)$ (line) with simulation for $T = 20$ (Blue), $T = 25$ (Green) and $T = 30$ (Red) and the number of samples $N = 10^6$. Parameter values are $\gamma = 1$, $\sigma = 1$, $x_0 = 0$ and $r = 2$.

results around the mean in both cases. Finding an average stretch far from the zero becomes exponentially unlikely so that the statistics of these rare events require simulations with a computationally inaccessible number of samples to be accurate. This explains the poor statistics far from the zero of the rate function.

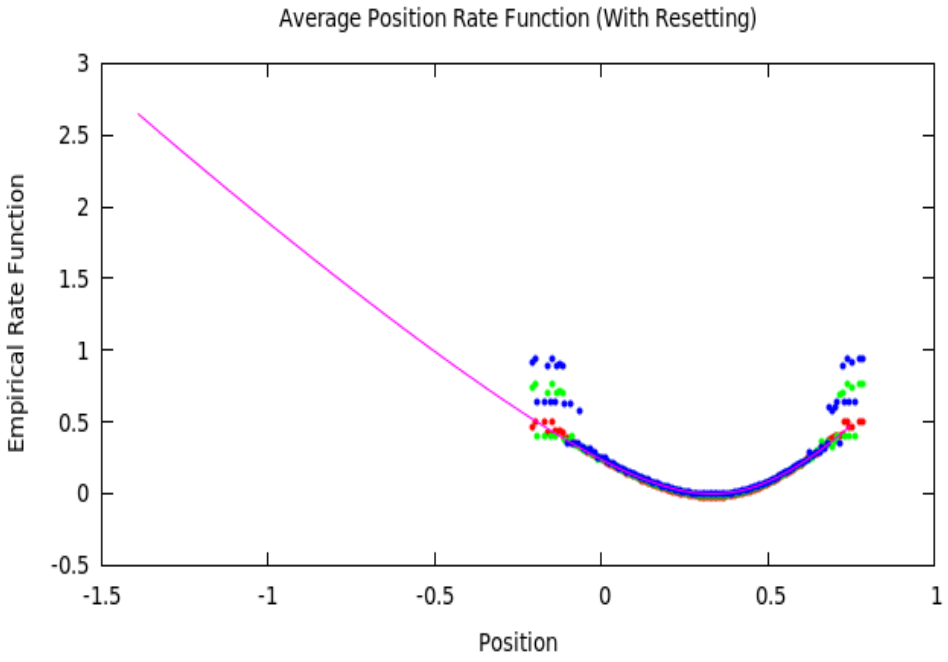

Figure 3.10: Comparison of $I_r(a)$ (line) with simulation for $T = 20$ (Blue), $T = 25$ (Green) and $T = 30$ (Red) and the number of samples $N = 10^6$. Parameter values are $\gamma = 1$, $\sigma = 1$, $x_0 = 0.5$ and $r = 2$.

3.4 Conclusion

In this section we have derived a general result that relates the Laplace transform of the generating function of additive observables undergoing a stochastic process with reset to the generating function for the same process without reset. We have used this result to study the mean behaviour and fluctuations of the stretch of a molecular motor modelled in a general way by a linear SDE called the Ornstein-Uhlenbeck process. We calculated the rate function for the integral of this process. The results obtained in this part will be the subject of a future publication together with H. Touchette and S. Sanbhapandit from the Raman Institute in Bangalore, India, who is a collaborator on this project.

To model N motors with a single filament this would have to be generalised so that the stretch of every motor follows an Ornstein-Uhlenbeck process. Moreover these N equations would all have to be coupled to an equation governing the dynamics of the filament. This makes the problem difficult as this equation would have to feedback into the evolution of each motor.

The following are other problems for which the reset results of this chapter could have applications.

To make the model for molecular motors more realistic we can include a time penalty each time the stretch is reset to account for the relaxation time of the motor tails when detaching.

Some motors switch between different types of diffusions, for example a

motor searching for a specific binding site along a DNA strand. It could be possible to use the idea of switching between different states as in Chapter 2 to model this.

Finally, an interesting problem not related to molecular motors is to repeat the calculation in this chapter for Brownian motion with reset. Since Brownian motion does not have a generating function for the additive observable of Eq. (3.3.2) we must use a different approach to the one in this chapter. There seems to be a trade-off of time scales in the case of Brownian motion with resetting. The time scale governing the resets contains the process so that one would expect a large deviation principle to arise but the one determining the growth of the observable undergoing pure diffusion between consecutive resets does not obey a large deviation principle.

Part II

Chapter 4

Dynamic networks

Before we can continue the second approach we must understand the developments that lead to a theory of dynamic networks. This entails doing a literature study of papers written on various subjects. The first is a paper by Jensen [35] which develops an approach to classical statistical dynamics using functional integrals. A similar paper was also written by Jouvet and Pythian [36]. This approach is more general than the Heisenberg operator type theory developed by Martin, Siggia and Rose (MSR) [37] as the MSR theory can be derived from the functional integral approach. Following this we start with some basic models for describing different types of polymers and show how one can transform a particle based theory to a field based theory. This will be done following the monograph on the equilibrium theory of Inhomogeneous Polymers by Fredrickson [38]. Next we discuss a paper by Edwards [39] which gives a field theoretic description of polymer networks to calculate the elastic free energy of the networks. This theory will here be introduced in the context of equilibrium systems, but we will make it dynamic later. Another paper that discusses this approach to elasticity is written by Deam and Edwards [40].

The ideas we introduce in this chapter will be applied in Chap. 5 to model a simple dynamic network consisting of many molecular motors and one filamentous ring.

4.1 Classical statistical dynamics

This section closely follows the paper by Jensen [35]. We can calculate statistical properties of classical statistical dynamics using a Heisenberg operator type theory. This was done by MSR and results in closed equations to calculate correlation and response functions. In the same way Feynman developed a path integral method for quantum mechanics it is possible to develop a functional integral theory for classical statistical dynamics. This theory is more general than the MSR theory since it is applicable to a broader range of nonlinear dynamical equations and can include non-Gaussian initial conditions,

multiplicative random forces and non-local interactions. The class of stochastic differential equations we would like to describe can be written generically as

$$\begin{aligned}\partial_{t_1}\psi(1) &= U_1(1) + U_2(12)\psi(2) + U_3(123)\psi(2)\psi(3) + \dots \\ &+ U_n(1\dots n)\psi(1)\dots\psi(n) + \delta(t_1 - t_0)\psi_0(\mathbf{1}). \end{aligned} \tag{4.1.1}$$

Here the fields $\psi(1)$ are real, multicomponent fields defined on $\mathbb{R}^{d+1}\times\mathbb{Z}^m$ where d gives the spatial dimensions and m gives the number of internal degrees of freedom. The variables are contained in

$$1 = (t_1, x_1, \dots, x_d, n_1, \dots, n_m) = (t_1, \mathbf{1}), \tag{4.1.2}$$

where t_1 is the time, the x_i's give the space variables and the internal degrees of freedom are given by the integers n_i. We shall use the notation where summation over repeated indices is implied.

The U_i's give the forces and interactions and are in general integrodifferential operators that can be written as a deterministic part and a stochastic part respectively

$$U_i(1\dots i) = \bar{U}_i(1\dots i) + \tilde{U}_i(1\dots i). \tag{4.1.3}$$

The initial condition, $\psi_0(\mathbf{1})$ can also be split in this way to include the possibility of random initial conditions.

We will be interested in calculating the mean fields $\langle\psi(1)\rangle$, fluctuation functions $\langle\psi(1)\psi(2)\rangle_c$ and response functions $R(12)$. The angled brackets are taken to mean the average over all random elements. The definitions for the fluctuation and response functions are respectively

$$\langle\psi(1)\psi(2)\rangle_c \equiv \langle\psi(1)\psi(2)\rangle - \langle\psi(1)\rangle\langle\psi(2)\rangle \tag{4.1.4}$$

$$R(12) = \left\langle \frac{\delta\psi(1)}{\delta\bar{U}(2)} \right\rangle \Bigg|_{\bar{U}(2)=0} \tag{4.1.5}$$

This type of stochastic differential equation (SDE) describes a large number of problems including but not limited to Navier-Stokes turbulence with a random stirring force, a particles motion in stochastic magnetic fields, stochastic wave equations and electromagnetic Vlasov turbulence.

The paper by Jensen shows that this entire class of SDEs can be described formally using the functional integral method. Before continuing it must be stated that the functional integral is defined but the general mathematical theory of these infinite dimensional integrals is not complete. Nevertheless the integrals have been used successfully for a long time. To define the functional integral the multidimensional space that the fields ψ are defined on must be discretised so that the index 1 now gives the position of a volume element of size ϵ^{d+1} on a lattice. The functional integral is the multiple integral at every

lattice point over the range of the field $\psi(i)$ in the limit as $\epsilon \to 0$ and is denoted by $[d\psi]$

$$\int [\mathrm{d}\psi] \ldots \equiv \lim_{\epsilon \to 0} \prod_i \int \mathrm{d}\psi(i) \tag{4.1.6}$$

where i takes values in the set of vertices.

For the rest of this section we will restrict ourselves to fields that only have a time dependence. It is possible to do the same for fields defined on multi-dimensional spaces but this mathematical complexity is trivial and obscures the important ideas. For the definition of the functional integral we had to discretise the space on which the fields are defined and must therefore write the SDE as a difference equation. This can be done in many different ways which all become equivalent in the limit as $\epsilon \to 0$. If $\psi(t)$ obeys an equation of the form of Eq. (4.1.1) we can consider any functional of $\psi(t)$

$$F[\psi] \equiv \int [\mathrm{d}\psi'] \quad \delta[\psi' - \psi] F[\psi'] \tag{4.1.7}$$

where ψ is the unique solution to Eq. (4.1.1), the δ is in this case the functional delta function defined in the usual way and we assume that the system is for the moment deterministic. The field is completely determined by the difference equation so that we can perform a change of coordinates

$$\begin{aligned} F[\psi] = \int [\mathrm{d}\psi'] \quad & \delta[\dot{\psi}'(1) - U_1(1) - U_2(12)\psi'(2) \ldots \\ & - U_n(1 \ldots n)\psi'(2) \ldots \psi'(n) - \delta(t_1 - t_0)\psi_0(\mathbf{1})] J[\psi'] F[\psi']. \end{aligned} \tag{4.1.8}$$

This enforces that the integral is non-zero only for the solution of Eq. 4.1.1. The Jacobian $J[\psi']$ depends on the choice of discretisation and since these all give the same result in the limit as $\epsilon \to 0$ we can pick

$$J = \prod_i \frac{1}{\epsilon} \tag{4.1.9}$$

where i runs over all lattice points. This is infinite in the limit $\epsilon \to 0$ but we will see later that this divergence will be cancelled out by another divergent constant. The next step is to write the delta functional in its Fourier representation

$$\begin{aligned} F[\psi] = c \int [\mathrm{d}\psi'][\mathrm{d}\hat{\psi}] \quad & \exp[-\hat{\psi}(1)(\dot{\psi}'(1) - U_1(1) - U_2(12)\psi'(2) \ldots \\ & - U_n(1 \ldots n)\psi'(2) \ldots \psi'(n) - \delta(t_1 - t_0)\psi_0(\mathbf{1}))] F[\psi'] \end{aligned} \tag{4.1.10}$$

where $c = \prod_i \frac{1}{2\pi\epsilon}$ and $\hat{\psi}$ is an imaginary field. By comparison with standard field theories we can write a Lagrangian $\mathcal{L}$ and a Hamiltonian $\mathcal{H}$

$$\begin{aligned} \mathcal{L} &\equiv \hat{\psi}(1)(\dot{\psi}'(1) - U_1(1) - U_2(12)\psi'(2) \ldots \\ &\quad - U_n(1 \ldots n)\psi'(2) \ldots \psi'(n) - \delta(t_1 - t_0)\psi_0(\mathbf{1})) && (4.1.11) \\ &\equiv \hat{\psi}\dot{\psi}' - \mathcal{H}[\psi', \hat{\psi}]. && (4.1.12) \end{aligned}$$

The randomness of the system can now be included again and we can easily average over random forces, interactions or initial conditions and write this as angled brackets. Since the random elements are all contained in the Lagrangian we have

$$\langle F[\psi]\rangle = c\int [\mathrm{d}\psi'][\mathrm{d}\hat{\psi}] \quad F[\psi']\langle\exp(-\mathcal{L})\rangle. \tag{4.1.13}$$

If we assume that the statistics of all the random elements are known the average can easily be performed so that we can define an effective Lagrangian L

$$\langle\exp(-\mathcal{L})\rangle \equiv \exp(-L) \tag{4.1.14}$$

from which we can write down statistical equations of motion. To calculate all the response and correlation function we define a generating functional that treats ψ and $\hat{\psi}$ equally

$$Z[\eta,\zeta] \equiv c\int [\mathrm{d}\psi'][\mathrm{d}\hat{\psi}] \quad e^{-L}\exp[\psi'(1)\eta(1)+\hat{\psi}(1)\zeta(1)]. \tag{4.1.15}$$

In most cases this will be too complicated to evaluate directly and numerous approximation techniques have been developed in quantum field theory to extract information from this expression. Examples of these methods are saddle point approximations and variational principles.

An alternative to evaluating the generating functional is finding evolution equations for the statistical quantities of interest. The first two give the evolution for the mean fields $\langle\psi\rangle$ and $\langle\hat{\psi}\rangle$

$$\frac{\langle\dot{\psi}(1)\rangle}{Z} - \frac{1}{Z}\left\langle\frac{\delta H}{\delta\hat{\psi}(1)}\right\rangle - \zeta(1) = 0 \tag{4.1.16}$$

$$-\frac{\langle\dot{\hat{\psi}}(1)\rangle}{Z} - \frac{1}{Z}\left\langle\frac{\delta H}{\delta\psi(1)}\right\rangle - \eta(1) = 0, \tag{4.1.17}$$

where the effective Hamiltonian is obtained from

$$\begin{aligned} H \equiv &\ln\langle\exp(\hat{\psi}(1))[U_1(1)+U_2(12)\psi'(2)\ldots \\ &+U_n(1\ldots n)\psi'(2)\ldots\psi'(n)+\delta(t_1-t_0)\psi_0(\mathbf{1})]\rangle. \end{aligned} \tag{4.1.18}$$

These are formally the Schwinger equations. We can derive the Dyson equations for the evolution of the correlation and response functions by taking functional derivatives of Eq. (4.1.16) to $\eta(2)$ and $\zeta(2)$

$$\langle\dot{\psi}(1)\psi(2)\rangle_c - \left[\left\langle\psi(2)\frac{\delta H}{\delta\hat{\psi}(1)}\right\rangle - \langle\psi(2)\rangle\left\langle\frac{\delta H}{\delta\hat{\psi}(1)}\right\rangle\right] = 0 \tag{4.1.19}$$

$$\langle\dot{\psi}(1)\psi(2)\rangle_c - \left[\left\langle\hat{\psi}(2)\frac{\delta H}{\delta\psi(1)}\right\rangle - \langle\hat{\psi}(2)\rangle\left\langle\frac{\delta H}{\delta\psi(1)}\right\rangle\right] = \delta(1-2). \tag{4.1.20}$$

We note here that the infinite constant c is no longer a problem since it appears in the numerator and the denominator so that the infinities cancel. The system of the Schwinger and Dyson equations can be closed using the method developed by MSR after which they describe exactly the mean fields, fluctuation functions and response functions of physical systems governed by equations of the form of Eq. (4.1.1). We must mention that there are calculation rules based on the interpretation of response functions, that enable a fulfilment of the Jacobian condition.

These equation describe a broader range of systems than the theory developed by MSR and using this formalism one can deal with systems that have non-Gaussian initial conditions, multiplicative random forces and non-local interactions.

4.2 Polymer field theory

For us to arrive at a field theoretic description of polymer networks we must first understand how polymers are modelled. This has been described many times in various pieces of literature and we will follow some of the chapters on the topic in the book by Fredrickson [38]. The first part of this section outlines some of the basic polymer chain models and the second illustrates how to transform a particle-based theory to a field theory.

The ideas of the following sections are for calculating equilibrium properties without any explicit dynamics. We will unify these equilibrium methods with the dynamic theory from before in Chap. 5.

4.2.1 Polymer chain models

The first model we consider is the freely jointed chain which considers a polymer made up of discrete points and links connecting these points. The points are numbered starting at 0 for the start of the polymer and going up to N at the end. The positions of the i^{th} point is given by the vector $\mathbf{r}_i$ so that a specific configuration can be defined by the set of point positions $R = \{\mathbf{r}_0, \mathbf{r}_1, \ldots, \mathbf{r}_N\}$. If we let the potential energy of a specific configuration be $U_0(R)$ we can write a partition function for a single chain

$$Z_0 = \int \mathrm{d}\mathbf{r}_0 \ldots \mathrm{d}\mathbf{r}_N \, e^{-\beta U_0(R)}. \tag{4.2.1}$$

This potential only contains short-range interactions in the case of an ideal chain where short range is in the sense of the distance along the polymer and not a spatially short ranged. Calculating the probability of finding a specific configuration is now easily done using

$$P_0(R) = \frac{1}{Z_0} e^{-\beta U_0(R)} \tag{4.2.2}$$

and ensemble averages for any function $f(R)$ of a configuration are given by

$$\langle f(R)\rangle_0 = \int \mathrm{d}\mathbf{r}_0 \ldots \mathrm{d}\mathbf{r}_N \, P_0(R) f(R). \tag{4.2.3}$$

The next model is known as the continuous Gaussian chain model and as the name suggests this considers the polymer to be continuous. It is used to describe flexible polymers that are continuous and linearly elastic. Instead of specifying a configuration by a set of vectors we use a vector valued function $\mathbf{r}(s)$ of the contour parameter $s \in [0, N]$. Note that s here is not the arc length along the polymer but rather indicates the infinitesimal parts of the polymer. This means that the stretch of the segments $\frac{d\mathbf{r}(s)}{ds}$ can fluctuate in magnitude. We can now write down what is known as the Edwards Hamiltonian in the literature

$$U_0[\mathbf{r}(s)] = \frac{3k_BT}{2b^2} \int_0^N ds \left| \frac{\mathrm{d}\mathbf{r}(s)}{\mathrm{d}s} \right|^2. \tag{4.2.4}$$

This is simply the potential energy of a specific configuration $\mathbf{r}(s)$ and is given here as a functional because it maps a continuous function to a number. The configurational partition function is almost the same as for the freely jointed chain model except that the integral is a functional one

$$\int [\mathrm{d}\mathbf{r}(s)] \, \exp(-\beta U_0[\mathbf{r}(s)]). \tag{4.2.5}$$

One way of defining the functional integral is using a generalized Fourier expansion. The configuration can be expressed in its spectral representation using the basis functions $\{\phi_0, \phi_1, \ldots\}$ as

$$\mathbf{r}(s) = \sum_{i=0}^{\infty} \mathbf{a}_i \phi_i(s). \tag{4.2.6}$$

If we choose the basis functions to be the cosine functions for example this becomes

$$\mathbf{r}(s) = \mathbf{a}_0 + 2\sum_{n=1}^{\infty} \mathbf{a}_n \cos\left(\frac{\pi n s}{N}\right) \tag{4.2.7}$$

which is a transformation that can be inverted since the cosine functions form an orthogonal basis to give the Rouse modes

$$\mathbf{a}_n = \frac{1}{N} \int_0^N \mathrm{d}s \, \cos\left(\frac{\pi n s}{N}\right) \mathbf{r}(s). \tag{4.2.8}$$

The functional integral can be interpreted as

$$\int [\mathrm{d}\mathbf{r}(s)] = \prod_{i=0}^{\infty} \int \mathrm{d}\mathbf{a}_i \tag{4.2.9}$$

and this can be used to calculate ensemble averages of functions of Rouse modes as

$$\langle f(\mathbf{a})\rangle_0 = \frac{\prod_{i=0}^{\infty}\int \mathrm{d}\mathbf{a}_i\, f(\mathbf{a})\exp(-\beta U_0(\mathbf{a}))}{\prod_{i=0}^{\infty}\int \mathrm{d}\mathbf{a}_i\, \exp(-\beta U_0(\mathbf{a}))} \tag{4.2.10}$$

The last model we will discuss is the Worm-like chain (WLC) model. The previous model was good to describe flexible polymers but in reality many polymers are semi-flexible. In this case we again describe the polymer configuration by a function $\mathbf{r}(s)$ but this time the variable $s \in [0, L]$ does give the arc length along the chain so that the length of the polymer L is constant. To model a semi-flexible polymer we need to include a contribution to the potential energy due to chain bending. We define the vector

$$\mathbf{u}(s) = \frac{\mathrm{d}\mathbf{r}(s)}{\mathrm{d}s} \tag{4.2.11}$$

and require $|\mathbf{u}(s)| = 1$ to encode the inextensibility of the polymer. The curvature of the polymer at a point s is given by the magnitude of $\frac{\mathrm{d}\mathbf{u}(s)}{\mathrm{d}s}$ so that our potential energy is the result of summing up the harmonic contributions of the bending at each point

$$U_0[\mathbf{u}(s)] = \frac{\lambda k_B T}{2}\int_0^L \mathrm{d}s \left|\frac{\mathrm{d}\mathbf{u}(s)}{\mathrm{d}s}\right|^2. \tag{4.2.12}$$

The configurational partition function is obtained as before where we have to remember to enforce the inextensibility constraint and the definition of $\mathbf{u}(s)$

$$Z_0 = \int [\mathrm{d}\mathbf{r}(s)] e^{-\beta U_0[\mathbf{u}(s)]} \prod_s \left[\delta\left(\mathbf{u}(s) - \frac{\mathrm{d}\mathbf{r}(s)}{\mathrm{d}s}\right)\delta(|\mathbf{u}(s)| - 1)\right]. \tag{4.2.13}$$

Working with this partition function directly is difficult due to the constraints but it is possible to reformulate this in a stochastic process analogy in dimensions higher than 2. The important point here is the method of constructing models for describing different types of polymers and how to enforce constraints.

4.2.2 A gas of particles

We now turn to the transformation needed to move from a particle based theory to a field theory. The effect is that the interactions particles have with each other are decoupled and replaced by interactions with auxiliary fields. We demonstrate how this is done using the basic example of a monatomic fluid. The canonical partition function for a fluid consisting of n identical particles confined to a volume V is

$$Z_c = \frac{1}{n!\lambda_T^{3n}}\int \mathrm{d}\mathbf{r}^n \quad \exp(-\beta U(\mathbf{r}^n)) \tag{4.2.14}$$

where $\lambda_T = \frac{h}{\sqrt{2\pi m k_B T}}$, h is the Planck constant, m is the mass of a single particle, k_B is the Boltzmann constant and T is the temperature. The potential $U(\mathbf{r}^n)$ is defined in various ways depending on the particular model one wants to study. We will take it to be a simple pair potential

$$U(\mathbf{r}^n) = \frac{1}{2}\sum_{j=1}^{n}\sum_{i\neq j}^{n} u(|\mathbf{r}_j - \mathbf{r}_i|) \tag{4.2.15}$$

where $u(|\mathbf{r}_j - \mathbf{r}_i|)$ is a pair potential whose form isn't important to illustrate the transformation. The first step is to rewrite the potential in terms of a density for the particle positions which we define as

$$\hat{\rho}(\mathbf{r}) = \sum_{i=1}^{n} \delta(\mathbf{r} - \mathbf{r}_i). \tag{4.2.16}$$

This enables us to write the potential energy as

$$U(\mathbf{r}^n) = \frac{1}{2}\int \mathrm{d}\mathbf{r} \int \mathrm{d}\mathbf{r}' \quad \hat{\rho}(\mathbf{r}) u(|\mathbf{r} - \mathbf{r}'|)\hat{\rho}(\mathbf{r}') - \frac{1}{2} n u(0). \tag{4.2.17}$$

The integrals in the first term include self-interactions for each of the n particles which is why in the second term these are subtracted. When plugging this into the partition function it becomes clear that the potential at $u(0)$ has no effect on the thermodynamics but only changes the reference chemical potential

$$Z_c = \frac{z_0^n}{n!}\int \mathrm{d}\mathbf{r}^n \exp\left(-\frac{\beta}{2}\int \mathrm{d}\mathbf{r}\int \mathrm{d}\mathbf{r}' \quad \hat{\rho}(\mathbf{r}) u(|\mathbf{r} - \mathbf{r}'|)\hat{\rho}(\mathbf{r}')\right) \tag{4.2.18}$$

where $z_0 = e^{\frac{\beta u(0)}{2}}/\lambda_T^3$. The second step is to insert the identity in the partition function in the following form

$$1 = \int [\mathrm{d}\rho] \quad \delta[\rho - \hat{\rho}] \tag{4.2.19}$$

and writing the delta functional in its Fourier representation

$$\delta[\rho - \hat{\rho}] = \int [\mathrm{d}\omega] \quad \exp\left(i\int \mathrm{d}\mathbf{r} \quad \omega(\mathbf{r})[\rho(\mathbf{r}) - \hat{\rho}(\mathbf{r})]\right) \tag{4.2.20}$$

where $\omega(\mathbf{r})$ is a real scalar field. The partition function becomes

$$\begin{aligned} Z_c = \frac{z_0^n}{n!}\int [\mathrm{d}\rho]\int [\mathrm{d}\omega]\int \mathrm{d}\mathbf{r}^n \quad \exp\Bigg(i\int \mathrm{d}\mathbf{r} \quad \omega(\mathbf{r})(\rho(\mathbf{r}) - \hat{\rho}(\mathbf{r})) \\ - \frac{\beta}{2}\int \mathrm{d}\mathbf{r}\int \mathrm{d}\mathbf{r}' \quad \rho(\mathbf{r}) u(|\mathbf{r} - \mathbf{r}'|)\rho(\mathbf{r}')\Bigg). \end{aligned} \tag{4.2.21}$$

All that remains to be done is performing the integral over all of the particle positions. To do this we note that the only part of the expression in the exponential that depends on the particle positions is $\exp(-i\int \mathrm{d}\mathbf{r}\omega\hat{\rho})$ and the integral over this is

$$\begin{aligned}\int \mathrm{d}\mathbf{r}^n \quad e^{-i\int \mathrm{d}\mathbf{r}\omega\hat{\rho}} &= \prod_{i=1}^{n}\int_V \mathrm{d}\mathbf{r}_i \quad e^{-i\omega(\mathbf{r}_i)} \\ &= (VZ_s[i\omega])^n \end{aligned} \tag{4.2.22}$$

where we have used the definition of the density $\hat{\rho}$ and $Z_s[i\omega]$ is the single particle partition function given by

$$Z_s[i\omega] \equiv \frac{1}{V}\int_V \mathrm{d}\mathbf{r} \quad e^{-i\omega(\mathbf{r})}. \tag{4.2.23}$$

The final partition function now written completely as a statistical field theory is

$$Z_c = \frac{(z_0V)^n}{n!}\int[\mathrm{d}\rho]\int[\mathrm{d}\omega] \quad \exp(-H[\rho,\omega]) \tag{4.2.24}$$

where the effective Hamiltonian is

$$\begin{aligned}H[\rho,\omega] = &-i\int \mathrm{d}\mathbf{r} \quad \omega(\mathbf{r})\rho(\mathbf{r}) + \frac{\beta}{2}\int \mathrm{d}\mathbf{r}\int \mathrm{d}\mathbf{r}' \quad \rho(\mathbf{r})u(|\mathbf{r}-\mathbf{r}'|)\rho(\mathbf{r}') \\ &- n\ln Z_s[i\omega]. \end{aligned} \tag{4.2.25}$$

This is only for the case of particles but a similar procedure can be used to do the same for polymers. This procedure of introducing densities for the particles is the first step when using a random phase approximation (RPA).

4.3 Field theoretic description of networks

In a network the cross-links are typically taken to be fixed. This means when calculating properties of the network it is necessary to think carefully about how to average over the different networks that can be formed. If the different networks are averaged over in the same way one averages over the thermal variables it is really a description of a network whose topology is constantly changing. The first subsection of this section deals with this difference in averaging that is needed and the second shows how Wick's theorem can be used to calculate how with what probability different network are realised.

4.3.1 Quenched averaging and the replica trick

When dealing with systems with disorder degrees of freedom two questions arise

- How are the different realisations of the disorder distributed?
- How does one average over the disorder sensibly?

In the case of networks the specific realisation of a network remains fixed so that treating the disorder degrees of freedom on the same level as the normal degrees of freedom does not make sense. The average that needs to be taken to consider the specific realisation of disorder as fixed is called an quenched average. This is in general not an easy average to calculate analytically and various ways have been developed to obtain information about the system from this average without calculating it explicitly. One of these methods is the replica trick. To illustrate this trick and more formally define what it means to take a quenched average we follow the chapter on the subject in the book by M. Mezard, G. Parisi and M. A. Virasoro entitled "*Spin glass theory and beyond*" [41].

Consider a system with Hamiltonian depending on normal degrees of freedom $\{x\}$ and disorder degrees of freedom $\{\delta\}$

$$H(\{x\},\{\delta\}). \tag{4.3.1}$$

An example of disorder degrees of freedom could be the set $\{\delta\}$ defining the specific topology of a rubber network that is a result of the manufacturing process. For each set $\{\delta\}$ we can calculate the partition function

$$Z(\{\delta\}) = \sum_{\{x\}} \exp(-\beta H(\{x\},\{\delta\})) \tag{4.3.2}$$

where $\beta = \frac{1}{k_B T}$. From this we can compute the free energy

$$F(\{\delta\}) = -\frac{1}{\beta N} \ln Z(\{\delta\}) \tag{4.3.3}$$

where N is the number of normal degrees of freedom. Standard statistical mechanics computes $F(\{\delta\})$ at a specific $\{\delta\}$ but often this specific disorder is not known. What might be known is the probability distribution, $P(\{\delta\})$ for the different disordered states. This distribution could depend on if the rubber was stirred or left to stand for a while for example (continuing the example from above).

Generally the distinction between the normal and disorder degrees of freedom comes from the fact that in many systems the changes in the disorder degrees of freedom occur on time scales that are very large in comparison to the ones typically associated with the normal degrees of freedom.

Before defining the quenched average it is worth mentioning that in these definitions it is assumed that the free energy is self-averaging meaning that it assumes the same value as N goes to infinity for all realisations of the $\{\delta\}$ that have a non-vanishing probability of occurring.

We will denote the quenched average by $\langle \ldots \rangle_\delta$ and define it for the free energy as

$$\bar{F} = \langle F(\{\delta\}) \rangle_\delta \equiv \sum_{\{\delta\}} P(\{\delta\}) F(\{\delta\}). \tag{4.3.4}$$

This is rather tricky to compute in most cases as opposed to calculating the annealed average for the free energy

$$\begin{aligned} F &= \ln \left[\sum_{\{\delta\}} P(\{\delta\}) \sum_{\{x\}} \exp(-\beta H(\{x\}, \{\delta\})) \right] \\ &= \ln[\langle Z(\{\delta\}) \rangle_\delta] \end{aligned} \tag{4.3.5}$$

where we can see that the $\{x\}$ and $\{\delta\}$ are treated in the same way. This means that the disorder and normal degrees of freedom are changing on the same time scale while in the quenched case the system is constrained to a specific disordered state but we average over our ignorance of what that state is.

One method of dealing with this is the replica trick. This essential idea of this method is to analytically continue the average of n replicas of the system with a specific disorder to calculate the average of the free energy by taking the limit as n goes to zero. It is assumed that the replicas do not interact with each other. To show how this is done we need to define

$$Z_n \equiv \sum_{\{\delta\}} P(\{\delta\}) (Z(\{\delta\}))^n \tag{4.3.6}$$

and

$$F_n \equiv -\frac{1}{\beta n N} \ln Z_n. \tag{4.3.7}$$

If n is small we can approximate Z_n as

$$Z_n \approx \sum_{\{\delta\}} P(\{\delta\})[1 + n \ln Z(\{\delta\})] = 1 + n \sum_{\{\delta\}} P(\{\delta\}) \ln Z(\{\delta\}) \tag{4.3.8}$$

where we have used the fact that the probability distribution for the disorder is normalised. Now since $\ln(1+x) \approx x$ when x is small

$$\begin{aligned} \lim_{n \to 0} F_n &= \lim_{n \to 0} \frac{-1}{\beta n N} \ln(1 + n \sum_{\{\delta\}} P(\{\delta\}) \ln Z(\{\delta\})) \\ &= \frac{-1}{\beta n N} n \sum_{\{\delta\}} P(\{\delta\}) \ln Z(\{\delta\}) \\ &= -\frac{1}{\beta N} \langle F(\{\delta\}) \rangle_\delta \\ &= -\frac{\bar{F}}{\beta N}. \end{aligned} \tag{4.3.9}$$

This means by taking the limit as n goes to zero of F_n we get the quenched average of the free energy. For a $n \in \mathbb{Z}$

$$(Z\{\delta\})^n = \sum_{\{x\}_1} \dots \sum_{\{x\}_n} \exp(-\beta \sum_{i=1}^{n} H(\{x\}_i, \{\delta\})) \tag{4.3.10}$$

where each set of $\{x\}_i$ is under the same disorder $\{\delta\}$. For a sensible quenched averaged free energy two limits need to be taken. The first is n to zero and the second is N to infinity. The second is for the free energy to be self-averaging. These averages should technically be taken in that order but in most cases the order can be reversed without problems occurring. The replica trick can be summarised in three steps

- define F_n for integers
- analytically continue F_n for $n \in \mathbb{R}$
- take the limit as n goes to zero of F_n to compute $\bar{F}$.

Mathematically this is maybe not the cleanest method but it has been applied very successfully in the literature and works well in the high temperature domain.

4.3.2 Wick's theorem for networks

This section takes us one step closer towards our dynamic network theory by developing a description of polymer networks using field theory as done by Sir. S. F. Edwards in 1988. The previous section discussed how one goes about defining a quenched average for networks using a probability distribution for the networks. This probability distribution is not always easy to calculate especially in the case where there are many cross-links. If one puts in the cross-linking constraints by hand the problem is a very tedious one. Edwards shows that it is possible to calculate this distribution using fields. The paper's aim is to use this formalism to calculate the elastic free energy concisely. The standard model used to describe cross-linked networks at the time had some problems as it treated all polymers to be Gaussian, could only describe systems with a functionality of four and took the lengths of the polymers between cross-links to be the same. We start by writing down the weight of a specific configuration

$$\exp\left[-\frac{3k_BT}{2l}\int_0^L \left(\frac{\partial r(s)}{\partial s}\right)^2 \mathrm{d}s\right] \tag{4.3.11}$$

where l is the Kuhn length, L is the length of the polymer, s gives the arc length along the polymer and $r(s)$ is the real space position of the polymer. To enforce cross-links we introduce delta functions. A cross-link between position

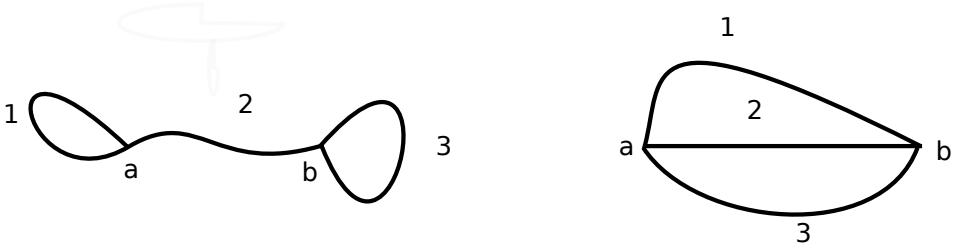

Figure 4.1: Two distinct topologies

s_i^i on the i^{th} and position s_j^ion the j^{th} chain can be written into the probability distribution as

$$\delta(r_i(s_i^i) - r_j(s_j^i)). \tag{4.3.12}$$

For illustration purposes let us consider a long polymer that has been cross-linked N times. The cross-linking constraint now becomes

$$\prod_{i=0}^{N} \delta(r(s_i) - r(s_i')) \tag{4.3.13}$$

where we have linked positions s_i along the polymer to position s_i'. Let us assume we have 3 polymers of length L and two cross-links with functionality 3. It is possible to form two topologically distinct networks which can be seen in figure 4.1. The two cross-linking positions are labelled by a and b and the three polymers by 1, 2 and 3.

If we want to write the partition function for the first network we must perform the following integral

$$\begin{aligned}\int [\mathrm{d}r_1(s)][\mathrm{d}r_2(s)][\mathrm{d}r_3(s)] \quad e^{-\beta H(r_1,r_2,r_3)} &\times \delta(r_1(0) - r_1(L)) \\ &\times \delta(r_3(0) - r_3(L)) \\ &\times \delta(r_1(0) - r_2(0)) \\ &\times \delta(r_2(L) - r_3(L))\end{aligned} \tag{4.3.14}$$

for the second we have

$$\begin{aligned}\int [\mathrm{d}r_1(s)][\mathrm{d}r_2(s)][\mathrm{d}r_3(s)] \quad e^{-\beta H(r_1,r_2,r_3)} &\times \delta(r_1(0) - r_2(0)) \\ &\times \delta(r_1(0) - r_3(0)) \\ &\times \delta(r_1(L) - r_2(L)) \\ &\times \delta(r_2(L) - r_3(L)).\end{aligned} \tag{4.3.15}$$

These need to be summed over all permutations of the polymers to give the final partition function. Clearly a more elegant way of realising all the possible networks is needed.

The theorem that allows us to do this rather elegantly is Wick's theorem. The following closely resembles the explanation of Wick's theorem given by Karl Möller in chapter 4.4.1 of his MSc thesis.

The theorem is essentially a generalisation of the integral

$$N\int_{-\infty}^{\infty}\mathrm{d}x \quad x^2 e^{-\frac{x^2}{2a}} = a \tag{4.3.16}$$

where N is just a normalization constant. The first generalisation is to a higher dimension using matrices with positive definite matrix $\mathbb{A}$ resulting in

$$N\int \mathrm{d}\vec{x} \quad x_i x_j \exp\left[\frac{-1}{2}\vec{x}^T\mathbb{A}^{-1}\vec{x}\right] = A_{ij}. \tag{4.3.17}$$

Following this we must assume that it is possible to take the number of indices of the vectors and matrix to infinity in such a way that the vectors become functions and the matrix when we take it as the identity becomes a delta function. This means of course that the integral over vectors becomes a functional integral

$$N\int [\mathrm{d}x] \quad x(t)x(t')\exp\left[-\frac{1}{2}\int_t x(t)x(t)\right] = \delta(t-t'). \tag{4.3.18}$$

The last step is to simply take the functions to be complex fields ϕ and $\phi^\star$. We can show that this results in three cases. Integrating the exponential multiplied by $\phi(t)\phi(t)$

$$N\int [\mathrm{d}\phi][\mathrm{d}\phi^\star] \quad \phi(t)\phi(t')\exp\left[-\frac{1}{2}\int_t \phi(t)\phi^\star(t)\right] = 0 \tag{4.3.19}$$

and similarly

$$N\int [\mathrm{d}\phi][\mathrm{d}\phi^\star] \quad \phi^\star(t)\phi^\star(t')\exp\left[-\frac{1}{2}\int_t \phi(t)\phi^\star(t)\right] = 0. \tag{4.3.20}$$

The last case is the exponential multiplied by $\phi(t)\phi^\star(t')$ which results in

$$N\int [\mathrm{d}\phi][\mathrm{d}\phi^\star] \quad \phi(t)\phi^\star(t')\exp\left[-\frac{1}{2}\int_t \phi(t)\phi^\star(t)\right] = \delta(t-t'). \tag{4.3.21}$$

If we are considering a product of fields say

$$S = \phi(t_1)\phi(t_2)\phi(t_3)\ldots\phi(t_n)\phi^\star(t'_1)\phi^\star(t'_2)\phi^\star(t'_3)\ldots\phi^\star(t'_m) \tag{4.3.22}$$

Wick's theorem states

$$N\int [\mathrm{d}\phi][\mathrm{d}\phi^\star] \quad S\exp\left[-\frac{1}{2}\int_t \phi(t)\phi^\star(t)\right] = \begin{cases} \sum_{\text{permutations}}\prod_{i<j}\delta(t_i - t'_j) & \text{if } m = n \\ 0 & \text{otherwise} \end{cases}.$$

If we take the fields to represent the polymers and the conjugate fields the cross-linking positions the integral will give us all possible networks with the polymers and cross-links given. If we want to create a network where cross-links have a higher functionality we can just take $(\phi^\star(R))^n$ where n is the functionality of the cross-link at position R.

We will take the fairly disconnected ideas introduced in this chapter and use them to build a dynamical theory of networks in the next chapter.

Chapter 5

Filamentous ring

In this section we outline a novel approach to dealing with a more complicated system consisting of the components of the previous sections. The system is not only mathematically solvable but also has physical relevance. For organisms to grow and stay healthy cells must constantly reproduce. This is done by the process of cell division. The cell must first duplicate the material inside needed for both daughter cells to survive. The duplication of the DNA requires optimal search dynamics that can be modelled using the idea of stochastic resetting from before. Our interest now is however the part of the cell division process known as cytokineses where the cell is physically divided in two. A ring consisting of many filaments is formed around the equator of the cell. At the same time active cross-links are formed between the filaments by molecular motors. These start pulling the filaments across each other by walking in opposite directions on parallel filaments. The effect is that the ring is contracted dividing the cell. The dynamics involved in this process are not well understood and we propose here a simplified model to investigate the effect of a dense motor distribution on the contraction speed.

5.1 Field-Theoretic approach to networks

We will later see that an interesting way of approaching the system described above is through field-theoretic network theory. This subject has been pioneered in the context of polymers by Sir S. Edwards of Cambridge [26]. Successful application of this theory has been wide spread in equilibrium situations where a network is permanently cross-linked. One of the corner stones of this theory is Wick's Theorem which is used to count all valid cross-linked configurations of the network. A very heuristic explanation of Wick's theorem in the context of network theory can be found in the previous chapter. The novel idea here is to have a dynamic network (formed between a single filament and many motors) that reforms at different points in time while evolving under the constraint of the Langevin equation for the different components of the

system. Similar ideas have been used by G. H. Fredrickson and E. Helfand [42] to investigate screening of hydrodynamic disturbances and elastic stress dynamics in polymer solutions.

5.2 Simplified model

Having many filaments with active cross-links and changing overlaps is fairly complex and is something being investigated in Stellenbosch by S. Pachong and Prof. K. K. Müller-Nedebock. For the purpose of our investigation we will consider one filament only interacting with many molecular motors attached by their tails to a underlying stationary ring. This reduces the problem to one dimension and eliminates many degrees of freedom that would have made the calculation an ambitious one for a MSc. In contrast to the continuous position variable describing the position of the molecular motor from previous section we have here discrete attachment sites along the filament. We assume these as well as the motors attached to the stationary ring to be uniformly distributed in space. The position of the filament can be described by an angle $\theta(t)$ and the position of individual attachment sites as the filament position plus a constant $\theta_n(t) + \frac{2\pi n}{N}$ for the n^{th} attachment site. (N is the total number of attachment sites.) For the motors we describe only the stretch $x_m(t)$ for the m^{th} motor (M is the total number of motors). The dynamics of the motor stretch are given by a Langevin equation

$$\gamma_M \dot{x}_m(t) = -kx_m(t) + f_M(t) \tag{5.2.1}$$

where we assume the motors are identical and so have the same spring constant k and friction coefficient γ_M. To relate the angle describing the filament to an actual physical position we need the radius of the ring R.

What makes this interesting is the attachment/detachment of the motors which need to be dealt with in a sensible way. We propose representing the motor heads and attachment sites as fields and conjugate fields. This way we can write a partition function that calculates all the networks that can be formed at each point in time. Once the network is formed we use the Langevin equations to describe the dynamics of the network for a time δt and then form a new network. This is not quite enough as we need to favour certain networks to encode the preferential direction of attachment for the motors. A wordy explanation of the mathematics is in this case less effective than letting the mathematics explain itself.

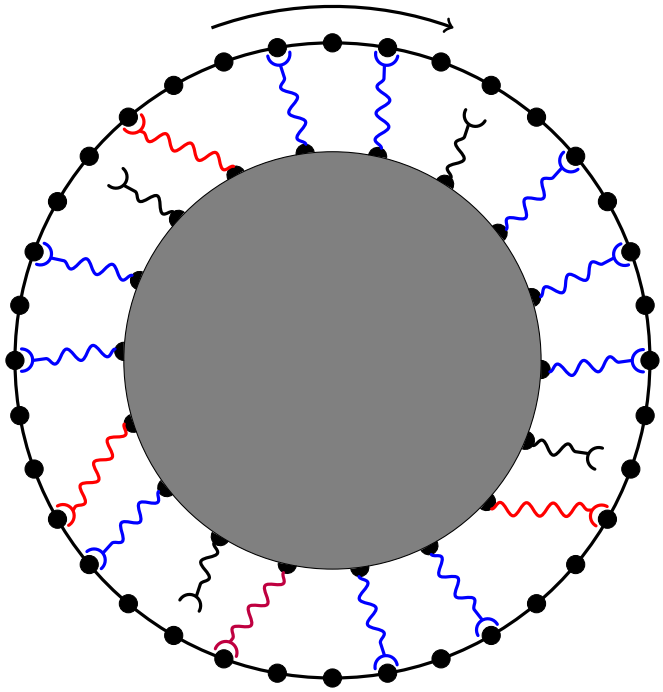

Figure 5.1: Visualisation of model

5.3 Dynamic network partition function

The partition function is given by

$$
\begin{aligned}
Z_f = &\int [\mathrm{d}\theta][\mathrm{d}\hat{\theta}][\mathrm{d}\phi][\mathrm{d}\phi^*] \prod_{m=1}^{M} \prod_t [\mathrm{d}x_m(t)][\mathrm{d}\hat{x}_m(t)] \\
&\times \exp\left[i \int_t \hat{\theta}(t)(-\gamma_\theta \dot{\theta} + f_\theta(t)) + i \int_t \sum_{m=1}^{M} \hat{x}_m(t)\left(-\gamma \dot{x}_m(t) + f_m(t)\right) \right] \quad (5.3.1) \\
&\times \exp\left[- \int_{v,r,t} \phi(v,r,t)\phi^*(v,r,t) \right] \\
&\times \prod_t \prod_{m=1}^{M} (1 - p(x_m,t) + p(x_m,t)\phi(v,r,t)) \prod_t \prod_{n=1}^{N} (1 + \phi^*(v,r,t)).
\end{aligned}
$$

The second line encodes the dynamics of the system when a network is formed and the third line counts all the possible networks. The fields ϕ and ϕ^* are the motor heads and attachment sites respectively. These fields depend position, velocity and time. The reason for this is that there are dynamics governing the motion of a motor along the filament. This means that there might be a relative velocity between filament and motor. We have seen that we produce delta function when performing integrals over these fields that match the arguments and so we can use this to match the velocity of the filament in the argument

of the field ϕ with a shifted velocity in the field ϕ^*. In this way the motion of the motor along the filament can be encoded.

Alternatively one can use $p(x_m, t)$ which is a suppression factor for networks where a motors tail is very extended and also favours networks with motor tails extended in the bias direction so that again the biased motion of the motor along the filament is enforced.

The product over the fields in the last line takes into account that not all motors are attached at all times. The choice of the product we have here will give us any number of attached motors because it will give us all possible combinations of fields with conjugate fields. The terms in the product where there are not an equal number of fields and conjugate fields are zero when integrated due to Wick's theorem. A sensible choice for the suppression factor is

$$p(x,t) = \mathcal{N} e^{-\frac{(x-x_0)^2}{2}} \tag{5.3.2}$$

where x_0 gives the average stretch and $\mathcal{N}$ is just a normalization factor. The dynamics of the system are encoded by the second line in the partition function and are enforced here by delta-functional constraints which we have written in their Fourier representation. At this point it seems as if the mathematical formalism is overkill considering the simplicity of the model and in fact the expression will keep getting more complicated in the next step. The reader is encouraged to persevere as the power of this formalism will soon become apparent. To simplify things we introduce two densities

$$\rho(v,r,t) = \sum_{m=1}^{M} \delta\left(r - x_m(t) - \frac{2\pi R m}{M}\right) \delta(v - \dot{x}_m(t)) \tag{5.3.3}$$

$$\rho_\theta(v,r,t) = \delta(v - \dot{\theta}(t)) \sum_{n=1}^{N} \delta\left(r - \theta(t) - \frac{2\pi R n}{N}\right) \tag{5.3.4}$$

so that we can write the last line of Eq. (5.3.1) as

$$\exp\left[\int_{v,r,t} [\rho \ln(1 + p(r)(\phi - 1)) + \rho_\theta \ln(1 + \phi^*) - \phi\phi^*]\right] \tag{5.3.5}$$

where we have suppressed the explicit dependence of ρ, ρ_θ and the ϕ's on r, v and t for clarity.

5.4 Saddle-point approximation

The exponential of Eq. (5.3.5) can be dealt with in a saddle-point approximation this means that we replace the full system by the dominant behaviour. This will give us an idea of how the system typically behaves. It is also a calculation that can be easily be extend to include the fluctuations around this

typical behaviour. What we would like to calculate is how the steady-state filament velocity depends on various system parameters.

Let

$$F = \int_{v,r,t} [\rho \ln(1 + p(r)(\phi - 1)) + \rho_\theta \ln(1 + \phi^*) - \phi\phi^*] \tag{5.4.1}$$

so that the saddle-point equations are

$$\left.\frac{\delta F}{\delta \phi}\right|_{\bar{\phi},\bar{\phi}^*} = 0 \qquad \text{and} \qquad \left.\frac{\delta F}{\delta \phi^*}\right|_{\bar{\phi},\bar{\phi}^*} = 0 \tag{5.4.2}$$

where the δ indicates that this is a functional derivative which is defined as

$$\frac{\delta F[\phi(\tau)]}{\delta \phi(t)} = \lim_{\epsilon \to 0} \left[F[\phi(\tau) + \epsilon\delta(\tau - t)] - F[\phi(\tau)]\right]. \tag{5.4.3}$$

For the first saddle-point equation we explicitly calculate the functional derivative

$$\begin{aligned}\frac{\delta F[\phi(v,x,t)]}{\delta \phi(v',x',t')} = \lim_{\epsilon \to 0} \int_{v,x,t} &[\rho \ln[1 - p + p\phi + \epsilon p\delta(v - v')\delta(x - x')\delta(t - t')] \\ &+ \rho_\theta \ln(1 + \phi^*) - (\phi + \epsilon\delta(v - v')\delta(x - x')\delta(t - t'))\phi^* \\ &- \rho \ln(1 - p + p\phi) - \rho_\theta \ln(1 + \phi^*) + \phi\phi^*]\end{aligned} \tag{5.4.4}$$

and Taylor expand the natural logarithm in ϵ

$$\begin{aligned}\ln[1 - p + p\phi + \epsilon p\delta(v - v')\delta(x - x')\delta(t - t')] \approx \ln(1 - p + p\phi) \\ + \epsilon \left(\frac{p\delta(v - v')\delta(x - x')\delta(t - t')}{1 - p + p\phi}\right).\end{aligned} \tag{5.4.5}$$

which, after some cancellations, doing the integrals over the delta-functions and evaluating at $\bar{\phi}$ and $\bar{\phi}^*$ results in

$$\frac{\rho p}{1 - p + p\bar{\phi}} - \bar{\phi}^* = 0. \tag{5.4.6}$$

Following the same procedure for the second saddle-point equation gives us

$$\frac{\rho_\theta}{1 + \bar{\phi}^*} - \bar{\phi} = 0. \tag{5.4.7}$$

Eqs. (5.4.6) and (5.4.7) can be combined to find a quadratic formula for $\bar{\phi}^*$

$$\bar{\phi}^{*^2}(1 - p) + \bar{\phi}^*(1 - p + p\rho_\theta - p\rho) - \rho p = 0 \tag{5.4.8}$$

which gives two solutions. To find which is physical we calculate how many cross-links occur on average over a long time. This is easily done by replacing

$p \to pe^g$ in front of the ϕ in Eq. (5.3.1). In this way every time a link is formed the integral will produce a e^g and if we derive to g and set $g = 0$ we find $\bar{n}$ (the number of cross-links that occur on average in time) which can be seen from

$$\frac{\partial}{\partial g}\left[e^{\int_{v,x,t}\ln(1-p+pe^g\phi)}\right]|_{g=0} = e^{\int_{v,x,t}\ln(1-p+p\phi)\rho}\int_{v,x,t}\frac{p\phi}{1-p+p\phi}\rho \tag{5.4.9}$$

therefore

$$\bar{n} \approx \frac{p\phi}{1-p+p\phi}\rho = \bar{\phi}\bar{\phi}^*. \tag{5.4.10}$$

Here the $\approx$ means in the sense of the saddle-point approximation.

5.5 Self-consistency calculation

What we have presented in this chapter is a novel way of thinking about active polymer networks that resulted in an almost overly complicated mathematical formulation. The question we have not answered yet is if it is at all useful. We have an expression for the average number of cross-links at long times which means we should be able to calculate the steady-state velocity of the filamentous ring $\bar{v}$ by using a basic Langevin equation

$$-\gamma_0\bar{v} = F = k\langle\bar{n}x\rangle \tag{5.5.1}$$

where by the angle brackets we mean

$$\langle\bar{n}x\rangle = \int_{x,v}\bar{n}x. \tag{5.5.2}$$

If we assume that $v \to \bar{v}$ we can approximate the densities by

$$\rho_\theta(v,x,t) \to \delta(\bar{v}-v) \tag{5.5.3}$$

$$\rho(v,x,t) \to C \tag{5.5.4}$$

where C is a constant. These make sense since the speed of the filament becomes $\bar{v}$ and we assume that the density of the motors is so high that it can be essentially regarded as a constant. The expression for $\bar{n}$ can be written in terms of densities as

$$\bar{n}(v,x,t) \approx \frac{\rho_\theta A}{2(1-p)+A} \tag{5.5.5}$$

where

$$A = -(1-\rho+p(\rho_\theta-\rho)) - \sqrt{(1-\rho+p(\rho_\theta-\rho))^2 - 4(1-p)\rho p}. \tag{5.5.6}$$

The v integral in Eq. (5.5.2) is difficult since we have delta functions in the denominator etc. This is however easily dealt with by writing the delta function as a limit and taking the limit after doing the integral. We write

$$\rho_\theta(v,x,t) \to \lim_{\epsilon\to 0} \begin{cases} 0 & v \le \bar{v} \\ \frac{1}{\epsilon} & \bar{v} \le v \le \bar{v}+\epsilon \\ 0 & \bar{v}+\epsilon \le v \end{cases} \tag{5.5.7}$$

and perform the v integral to find

$$\int_v x\bar{n} = \lim_{\epsilon\to 0} \frac{xA|_{\rho_\theta=\frac{1}{\epsilon}}}{2(1-p)+A|_{\rho_\theta=\frac{1}{\epsilon}}}. \tag{5.5.8}$$

Taking the limit on the right gives us x. The x integral has bounds $-\pi R$ to πR so that this will be zero. This means to first order the filament will have a steady-state velocity of zero. There is however some more information to be obtained here. We can expand Eq. (5.5.8) in ϵ and see if the second and third order contributions give any insight. We also replace p with the biased choice from before

$$p = e^{-\frac{(x-x_0)^2}{2}} \tag{5.5.9}$$

and we treat ρ as a constant. The expansion is

$$x+\left(-1+e^{\frac{1}{2}(x_0-x)^2}\right)x\epsilon+x\left(1-e^{\frac{1}{2}(x_0-x)^2}-\rho+e^{(x_0-x)^2}\rho\right)\epsilon^2+O[\epsilon]^3. \tag{5.5.10}$$

The integral of the ϵ order term gives

$$\begin{aligned}\int_x \left(-1+e^{\frac{1}{2}(x_0-x)^2}\right)x = e^{\frac{1}{2}(x_0-\pi R)^2}&\left(1-\sqrt{2}x_0\text{DawsonF}\left[\frac{x_0-\pi R}{\sqrt{2}}\right]\right.\\ &\left.+\,e^{2x_0\pi R}\left(-1+\sqrt{2}x_0\text{DawsonF}\left[\frac{x_0+\pi R}{\sqrt{2}}\right]\right)\right)\end{aligned} \tag{5.5.11}$$

which we have plotted in Fig. 5.2 as a function of R with $x_0 = 0.001$. The order ϵ^2 terms integral gives

$$\begin{aligned}\int_x x\left(1-e^{\frac{1}{2}(x_0-x)^2}-\rho+e^{(x_0-x)^2}\rho\right) = \frac{1}{2}&e^{(x_0-\pi R)^2}\rho\,(1-2x_0\text{DawsonF}[x_0-\pi R]\\ &+\,e^{4x_0\pi R}\{-1+2x_0\text{DawsonF}[x_0+\pi R]\})\\ &+\,e^{\frac{1}{2}(x_0-\pi R)^2}\left(-1+\sqrt{2}x_0\text{DawsonF}\left[\frac{x_0-\pi R}{\sqrt{2}}\right]\right.\\ &\left.+\,e^{2x_0\pi R}\left(1-\sqrt{2}x_0\text{DawsonF}\left[\frac{c+\pi R}{\sqrt{2}}\right]\right)\right)\end{aligned} \tag{5.5.12}$$

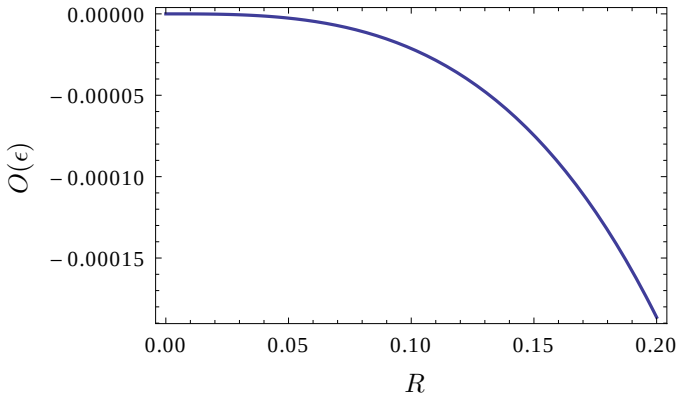

Figure 5.2: Order ϵ integral

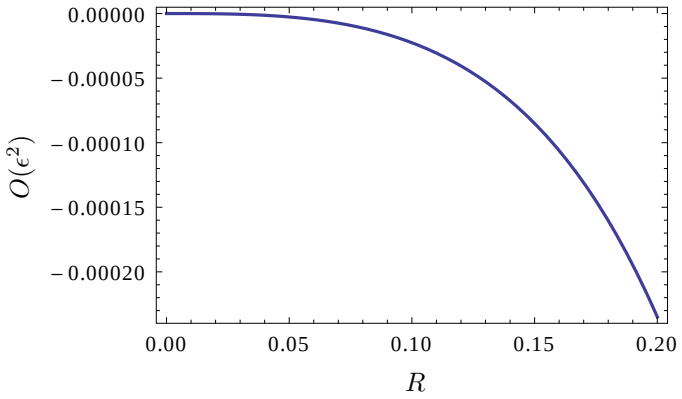

Figure 5.3: Order ϵ^2 integral

and is plotted in Fig. 5.3 with the same constants as before and $\rho = 1$.

This shows that the speed at which the ring rotates becomes larger as the radius of the ring is increased while keeping the density of motors constant. In the limit where ϵ is zero the velocity is also zero. This means we need to allow the filament to take a velocity in a small range around the steady state velocity, i.e. keep ϵ small but not zero.

We have shown that the bias motion of the motors can be included mathematically, at second order in ϵ at least, using a suppression factor for unfavourable networks. In addition to this we have formally included the attaching and detaching of molecular motors to and from the filament in our partition function by counting networks where not all motors are attached and allowing the network to reform dynamically.

Chapter 6

Conclusion and outlook

In this thesis we have considered systems consisting of molecular motors and filaments and described them using two different approaches. The focus was on including the attachment and detachment dynamics of individual motors in different mathematical formalisms and studying the mean behaviour as well as fluctuations around it in various limits.

In chapter 2 we have approximated molecular motors as stiff springs so that they switch between two states only. This allowed us to apply the methods of large deviation theory to study the long time fluctuations of a single motor as well as the behaviour of multiple motors when the number of motors is large. We have found the large deviation rate function for both of these cases, which characterises both the mean behaviour as well as the fluctuations. For the case of the many motor large deviations we have investigated the effect of taking different initial conditions.

In the third chapter we considered a single motor and showed that the attachment and detachment dynamics can be included explicitly in the stochastic differential equation describing the motion of the motor along the filament (Ornstein-Uhlenbeck process) using the notion of stochastic resetting. We used a renewal argument to find a relation between the generating function of additive observables with reset to the one without. We then used this result to find the rate function for the average motor stretch in time for a motor undergoing an Ornstein-Uhlenbeck process with resetting. We explored how the rate function changes when changing various system parameters for example the resetting position and the resetting rate. We compared the results with computer simulations and found excellent agreement between the two. The results of this section will be the topic of a future publication.

The last section of chapter 3 mentions the open problem of calculating the large deviation rate function for Brownian motion with resetting. This turns out to be non-trivial since the average position in time for Brownian motion does not have a rate function. This should be explored further and poses a very interesting and challenging problem.

In the context of motility assays it would be interesting to generalized

Chapter 3 to a many motor system where each motor undergoes a diffusion process but all of the motors are coupled to an equation governing the motion of a single filament.

Another interesting and physically relevant problem would be to make the resetting rate stretch dependent to encode the dependence of motor detachment on the load. Stretch dependent resetting rates have been studied for the case where we consider only the motor position (done in the context of search strategies) and not when considering the average motor stretch, which is a better indicator of the force the motor exerts on the filament over time.

One of the assumptions when using the approach of chapter 3 is that the motor detaches, relaxes and reattaches to the filament at zero stretch instantaneously. In reality, motors will take some time to relax and might not be able to reattach immediately after relaxing. This could be included by introducing a time penalty whenever a reset occurs that depends on how stretched the motor was at the time of detachment.

Further research could ask whether it would be possible to use the ideas of random evolutions (as spoken about in chapter 2) as well as the ideas of resetting to model this switching between modes of searching. In DNA searches, for example, a searcher protein switches between different searching modes. The one may be a careful search very close to the DNA and another may be a quick searching mechanism that moves the protein very quickly to another part of the DNA molecule.

In the second part of the thesis, starting with chapter 4, we considered a completely different type of mathematics used to study the interactions of filaments and molecular motors. Before introducing new ideas we reviewed the work that is needed to describe dynamics polymer networks. In chapter 5 we explore the used the methods from the previous chapter to describe a simple network. The network consisted of a filamentous ring being rotated by molecular motors attached to a circular substrate. Since the motors are detaching and attaching constantly we cannot have all the motors attached to the filament at each point in time. To take into account all the possible networks from those where no motors are attached to those where all motors are attached we used a specific product of the fields representing motor head and attachment site positions in the partition function. In this product we included a suppression factor $p(x_m, t)$, which is one of the ways to encode the bias of motors to move in a specific direction. We did this by making networks where motors are extended in the biased direction more likely than ones where they are not.

We used a saddle-point approximation to calculate the average number of attachments in time. This we used to calculate the steady-state velocity of the filament self-consistently as a function of various system parameters like the radius of the ring or the typical stretch of a single motor. The outcomes of this section are not the results of calculations but the new ideas of how to encode the attachment and detachment of molecular motors using a specific

product of fields and the biased motor motion by a suppression factor in this product rather than in the dynamical constraints.

To extend this work we could include the first-order field fluctuations in the saddle-point calculation. Alternatively one could include the stochastic part of the motor and filament dynamics. This might give a more interesting result for the steady-state velocity of the filament where we see that there is an optimal set of parameters for which the ring rotates with a maximal velocity. This can also be extended by using different functions for the motor and attachment site position densities or a different suppression factor $p(x_m, t)$.

Appendices

Appendix A

Introduction to large deviation theory

We present in this appendix the main elements of large deviation theory used in Chapter 2 and 3. Our presentation follows closely the review paper [43].

A.1 Large deviation principle

A random variable A_T is said to obey a large deviation principle (LDP) if the limit

$$\lim_{T\to\infty} -\frac{1}{T}\ln P(A_T = a) = I(a) \tag{A.1.1}$$

exists. Here $P(A_T = a)$ is the probability that A_T takes the value a and $I(a)$ is called the rate function. If this principle is obeyed we can approximate the probability by

$$P(A_T = a) \approx e^{-TI(a)} \tag{A.1.2}$$

which just gives the dominant behaviour of the probability as a decaying exponential.

A.2 The Gärtner-Ellis Theorem

We define the scaled cumulant generating function (SCGF) of A_T as

$$\lambda(k) = \lim_{T\to\infty} \frac{1}{T}\ln\langle e^{TkA_T}\rangle \tag{A.2.1}$$

where $k \in \mathbb{R}$. The theorem of Gärtner and Ellis states that:

If $\lambda(k)$ exists and is differentiable $\forall k \in \mathbb{R}$ then A_T obeys a large deviation principle (LDP) with rate function

$$I(a) = \sup_{k\in\mathbb{R}}\{ka - \lambda(k)\}. \tag{A.2.2}$$

Equation (A.2.2) is called the Legendre-Fenchel transform of $\lambda(k)$.

A.3 Properties of λ and I

We list some useful properties of the rate function and the SCGF (proved in [43])

- $\lambda(0) = 0$
- $\lambda(k)$ is always convex by definition
- Legendre duality: the slope of λ at k is the point at which the slope of I is k.
- $I(a) \geq 0 \ \forall a$.

These properties will be important for us to check many of our results.

A.4 Large deviations for stochastic differential equations

Consider a general stochastic differential equation (SDE)

$$dX_t = F(X_t)dt + \sigma dW_t \tag{A.4.1}$$

where the function $F(X_t)$ gives the deterministic part and the dW_t a Brownian motion giving the diffusive part. The generator of the process can be shown to be

$$L = F(x)\frac{d}{dx} + \frac{\sigma^2}{2}\frac{d^2}{dx^2}. \tag{A.4.2}$$

If we are interested in a random variable of the form

$$A_T = \frac{1}{T}\int_0^T f(X_t)dt \tag{A.4.3}$$

the SCGF is given by

$$\lambda(k) = \xi_{max}(L_k) \tag{A.4.4}$$

where ζ denotes the dominant eigenvalue of the tilted operator L_k such that

$$L_k\phi(x) = \lambda(k)\phi(x). \tag{A.4.5}$$

The tilting is done depending on the observable in question as follows

$$L_k = L + kf(x). \tag{A.4.6}$$

We note that L and L_k are not in general hermitian due to the $F(x)\frac{d}{dx}$ part in Eq. (A.4.2), which means that they have different left and right eigenvalues in general.

Appendix B

Modified Fokker-Planck equation

We give the proof of the modified Fokker-Planck equation, Eq. (3.1.4), for the diffusion process with resetting. For simplicity we consider a basic diffusion process without drift but the argument is similar for other diffusive processes.

We start by writing down the general master equation obtained by discretizing the line into intervals of size Δx

$$\partial_t p(n\Delta x, t) = \sum_{m=-\infty}^{\infty} [p(m\Delta x, t)w(m\Delta x \to n\Delta x) - p(n\Delta x, t)w(n\Delta x \to m\Delta x)] \tag{B.0.1}$$

where the probability density of finding the diffusing particle at position $n\Delta x$ at time t is given by $p(n\Delta x, t)$ and the transition rates by $w(m\Delta x \to n\Delta x)$. In Eq. (B.0.1) m and n give the position on the discretized space line. Since Brownian motion describes a simple random walk in space when space is discretized, it is enough to only consider transitions between neighbouring space positions. Then, to include reset each rate has to be modified with the possibility of the particle making a transition to the reset position which we take to be $\alpha\Delta x$. This results in transition rates of the form

$$w(n\Delta x \to m\Delta x) = \frac{1}{\Delta x^2}(\delta_{n,m+1} + \delta_{n,m-1}) + r\delta_{n,\alpha} \tag{B.0.2}$$

where we have used a constant resetting rate r. Substituting these rates into the discrete master equation gives

$$\begin{aligned}\partial_t p(n\Delta x, t) = \frac{1}{\Delta x^2}[p((n+1)\Delta x, t) + p((n-1)\Delta x, t) - 2p(n\Delta x, t)] \\ - rp(n\Delta x, t) + r\delta_{n,\alpha} \sum_{m=-\infty}^{\infty} p(m\Delta x, t).\end{aligned} \tag{B.0.3}$$

The sum in the last term is proportional to Δx^{-1} due to normalization of the probability density function.

The limit needed to produce the continues Fokker-Planck equation is $\Delta x \to 0$ while keeping $n\Delta x = x$. To calculate the limit we Taylor expand

$$\begin{aligned} p(x+\Delta x,t) &= p(x,t) + \partial_x p(x+\Delta x,t)|_{\Delta x=0}(\Delta x) \\ &\quad + \frac{1}{2}\partial_x^2 p(x+\Delta x,t)|_{\Delta x=0}(\Delta x)^2 + \dots \qquad \text{(B.0.4)} \\ p(x-\Delta x,t) &= p(x,t) - \partial_x p(x+\Delta x,t)|_{\Delta x=0}(\Delta x) \\ &\quad + \frac{1}{2}\partial_x^2 p(x+\Delta x,t)|_{\Delta x=0}(\Delta x)^2 + \dots \qquad \text{(B.0.5)} \end{aligned}$$

following the Kramer-Moyal expansion and recall that

$$\lim_{\Delta x\to 0} \frac{\delta_{n\Delta x,\alpha\Delta x}}{\Delta x} = \delta(x-x_0). \qquad \text{(B.0.6)}$$

From this we obtain the modified Fokker-Planck equation Eq. (3.1.4) previously found in [34]

$$\partial_t p(x,t) = \frac{\partial^2 p(x,t)}{\partial x^2} - rp(x,t) + r\delta(x-x_0). \qquad \text{(B.0.7)}$$

Appendix C

Eigenvalues and eigenfunctions of the Ornstein-Uhlenbeck generator

In this appendix we calculate the eigenvalues and eigenfunctions of the tilted generator of the Ornstein-Uhlenbeck process using a symmetrization procedure.

The random variable that we consider is

$$A_T = \frac{1}{T}\int_0^T X_t dt \tag{C.0.1}$$

such that our tilted generator is given by

$$L_k = L + kx = -\gamma x\frac{d}{dx} + \frac{\sigma^2}{2}\frac{d^2}{dx^2} + kx. \tag{C.0.2}$$

We want to solve the equation

$$L_k r_{k,i}(x) = \lambda_i(k) r_{k,i}(x). \tag{C.0.3}$$

L_k is not hermitian but it is possible to transform it to a hermitian operator using a unitary transformation. This is called a symmetrization and the resulting operator has the form

$$H = \sqrt{\rho} L_k \frac{1}{\sqrt{\rho}}. \tag{C.0.4}$$

Here ρ is the stationary distribution of the Fokker-Planck equation Eq. (3.1.2) which we write as

$$\rho = e^{-\phi} \tag{C.0.5}$$

where the "potential" ϕ is defined by ρ.

Assuming that $\phi(x)$ is twice differentiable we calculate the following commutators, which we need to calculate the symmetrized operator H:

- $\left[L_k^\dagger, e^{-\frac{\phi}{2}}\right] = \gamma x \left[\frac{d}{dx}, e^{-\frac{\phi}{2}}\right] + \frac{\sigma^2}{2}\left[\frac{d^2}{dx^2}, e^{-\frac{\phi}{2}}\right]$

- $\left[\frac{d}{dx}, e^{-\frac{\phi}{2}}\right] = -\frac{1}{2}e^{-\frac{\phi}{2}}\frac{d\phi}{dx}$
- $\left[\frac{d^2}{dx^2}, e^{-\frac{\phi}{2}}\right] = \frac{1}{4}e^{-\frac{\phi}{2}}\left(\frac{d\phi}{dx}\right)^2 - \frac{1}{2}e^{-\frac{\phi}{2}}\frac{d^2\phi}{dx^2} - e^{-\frac{\phi}{2}}\frac{d\phi}{dx}\frac{d}{dx}$.

The † denotes the adjoint yielding

$$L_k^\dagger = \gamma(1 + x\frac{d}{dx}) + \frac{\sigma^2}{2}\frac{d^2}{dx^2} + kx. \tag{C.0.6}$$

Using the definition of ρ for the Ornstein-Uhlenbeck process we find

$$\phi = \frac{\gamma x^2}{\sigma^2} \tag{C.0.7}$$

and from the commutation relations from above we find

$$H = \frac{\sigma^2}{2}\frac{d^2}{dx^2} - \frac{\gamma^2 x^2}{2\sigma^2} + \frac{\gamma}{2} + kx. \tag{C.0.8}$$

This is just a Schrödinger type operator since it is hermitian. It has the form

$$H_k = \frac{\sigma^2}{2}\frac{d^2}{dx^2} - V_k(x) \tag{C.0.9}$$

where

$$V_k(x) = \frac{\gamma^2 x^2}{2\sigma^2} - \frac{\gamma}{2} - kx \tag{C.0.10}$$

is an effective potential. This is the harmonic oscillator but with the potential shifted and multiplied by -1. We can find its minimum and the point at which this happens by completing the square

$$V_k(x) = \frac{\gamma}{2\sigma^2}(x - x^*)^2 - \frac{k^2\sigma^2}{2\gamma^2} - \frac{\gamma}{2} \tag{C.0.11}$$

with $x^* = \frac{k\sigma^2}{\gamma^2}$ being the the x-value where the minimum occurs. To match this with the quantum version of the harmonic oscillator we identify

- $\hbar \to \sigma$
- $m\omega \to \frac{\gamma}{\sigma}$
- $-mE_n \to \lambda_i$.

From the identifications and the fact that the eigenvalue spectrum should be shifted in the same way as the potential we find

$$\lambda_i(k) = \frac{k^2\sigma^2}{2\gamma^2} - i\gamma \tag{C.0.12}$$

and

$$r_{k,i}(x) = A_{r,i} H_i\left(\frac{\sqrt{\gamma}x}{\sigma} - \frac{k\sigma}{\gamma^{3/2}}\right) \exp\left[\frac{kx}{\gamma} - \frac{3k^2\sigma^2}{4\gamma^3}\right] \tag{C.0.13}$$

with the H_i's being the Hermite polynomials and $i = 0, 1, 2, \ldots$. Here

$$A_{r,i} = \frac{(-1)^i \gamma^{-\frac{3i}{2}} k^i \sigma^i}{\sqrt{2^n n!}\sqrt{(2n)!!}}. \tag{C.0.14}$$

List of References

[1] Selvin, P.: http://news.illinois.edu/news/04/0830myosim.atml.

[2] Robinson, W.B.: http://zorknot.com/2011/07/molecular-motors/.

[3] Marchetti, M.C., Joanny, J.-F., Ramaswamy, S., Liverpool, T.B., Prost, J., Rao, M. and Aditi Simha, R.: Hydrodynamics of soft active matter. *Rev. Mod. Phys.*, vol. 85, pp. 1143–1189, 2013.

[4] Guerin, T., Prost, J. and Joanny, J.-F.: Dynamic instabilities in assemblies of molecular motors with finite stiffness. *Phys. Rev. Lett.*, vol. 104, no. 248102, pp. 1–4, 2010.

[5] Gilboa, B., Gillo, D., Farago, O. and Bernheim-Groswasser, A.: Bidirectional cooperative motion of myosin-II motors on actin tracks with randomly alternating polarities. *Soft Matter*, vol. 5, pp. 2223–2231, 2009.

[6] Gur, B. and Farago, O.: Biased transport of elastic cytoskeletal filaments with alternating polarities by molecular motors. *Phys Rev. Lett.*, vol. 104, no. 238101, pp. 1–4, 2010.

[7] Dharan, N. and Farago, O.: Duty ratio of cooperative molecular motors. *Phys. Rev. E*, vol. 85, no. 021904, pp. 1–6, 2012.

[8] Guerin, T., Prost, J., Martin, P. and Joanny, J.-F.: Coordination and collective properties of molecular motors: theory. *Curr. Opinion Cell Bio.*, vol. 22, pp. 14–20, 2010.

[9] Banerjee, S., Marchetti, M.C. and Müller-Nedebock, K.K.: Motor-driven dynamics of cytoskeletal filaments in motility assays. *Phys. Rev. E*, vol. 84, no. 011914, pp. 1–11, 2011.

[10] Kusmierz, L., Majumdar, S.N., Sabhanpandit, S. and Schehr, G.: First order transition for the optimal search time of Lévy flights with resetting. *Phys. Rev. Lett.*, vol. 113, no. 220602, pp. 1–5, 2014.

[11] Vishwanathan, G., da Luz, M.G.E., Roposo, E.P. and Stanley, H.E.: *The Physics of Foraging.* Cambridge University Press, Cambridge, 2011.

[12] Benichou, O., Loverdo, C., Moreau, M. and Voituriez, R.: Intermittent search strategies. *Rev. Mod. Phys.*, vol. 83, no. 81, 2011.

[13] Boyer, D. and Solis-Salas, C.: Random walks with preferential relocations to places visited in the past and their application to biology. *Phys. Rev. Lett.*, vol. 112, no. 240601, 2014.

[14] Lovasz, L.: Combinatorics. *Bolyai Society for Mathematical Studies, Budapest*, vol. 2, p. 1, 1996.

[15] Montanari, A. and Zecchina, R.: Optimizing searches via rare events. *Phys. Rev. Lett.*, vol. 88, no. 178701, 2002.

[16] Konstas, I., Stathopoulos, V. and Jose, J.M.: Proc. 32nd Int. ACM SIGIR Conf. p. 195. ACM, New York, 2009.

[17] Kussel, E. and Leibler, S.: Phenotypic diversity, population growth, and information in fluctuating environments. *Science*, vol. 309, no. 2075, 2005.

[18] Kussel, E., Kishony, R., Balaban, N.Q. and Leibler, S.: Bacterial persistence: A model of survival in changing environments. *Genetics*, vol. 169, no. 1807, 2005.

[19] Reingruber, J. and Holcman, D.: Gated narrow escape time for molecular signaling. *Phys. Rev. Lett.*, vol. 103, no. 148102, 2009.

[20] Visco, P., Allen, R.J., Majumdar, S.N. and Evans, M.R.: Switching and growth for microbial populations in catastrophic responsive environments. *Biophys. J.*, vol. 98, no. 1099, 2010.

[21] Reingruber, J. and Holcman, D.: Transcription factor search for a DNA promoter in a three-state model. *Phys. Rev. E*, vol. 84, 2, no. 020901, 2011.

[22] Pakes, A.G.: Killing and resurrection of Markov processes. *Commun. Statist. - Stochastic Models*, vol. 13, no. 2, pp. 255–269, 1997.

[23] Di Crescenzo, A., Giorno, V., Nobile, A.G. and Ricciardi, L.M.: A note on birth-death processes with catastrophes. *Stat. Prob. Lett.*, vol. 78, pp. 2248–2257, 2008.

[24] Renshaw, E. and Chen, A.: Birth-death processes with mass annihilation and state-dependent immigration. *Commun. Statist. - Stochastic Models*, vol. 13, no. 2, pp. 239–253, 1997.

[25] Möller, K.: Dynamics of an active crosslinker on a chain and aspects of the dynamics of polymer networks. *MSc Thesis, Stellenbosch University*, 2011.

[26] Doi, M. and Edwards, S.: *The theory of polymer dynamics.* Clarendon Press, Oxford, 1988.

[27] Griego, R. and Hersh, R.: Theory of random evolutions wit applications to partial differential equations. *Trans. Am. Math. Soc.*, vol. 156, pp. 405–418, 1971.

[28] Hersh, R.: The birth of random evolutions. *Math. Intelligencer*, vol. 25, no. 1, pp. 53–60, 2003.

[29] Swischuck, A.: Random evolutions: A survey of results and problems since 1969. *Random Op. and Stoch. Eq.*, , no. 3, 1991.

[30] Kac, M.: Some stochastic problems in physics and mathematics. *Colloquium lectures in the pure and applied sciences*, vol. No. 2, 1956.

[31] Evans, M.R. and Majumdar, S.N.: Diffusion with optimal resetting. *J. Phys. A: Math Theor.*, vol. 44, no. 435001, 2011.

[32] Evans, M.R. and Majumdar, S.N.: Diffusion with resetting in arbitrary spatial dimension. *J. Phys. A: Math Theor.*, vol. 47, no. 285001, 2014.

[33] Majumdar, S.N., Sabhapandit, S. and Schehr, G.: Dynamical transition in the temporal relaxation of stochastic processes under resetting. *Phys. Rev. E*, vol. 91, no. 052131, 2015.

[34] Evans, M.R. and Majumdar, S.N.: Diffusion with stochastic resetting. *Phys. Rev. Lett.*, vol. 106, no. 160601, pp. 1–4, 2011.

[35] Jensen, R.: Functional integral approach to classical statistical dynamics. *J. Stat. Phys.*, vol. 25, no. 2, pp. 183–210, 1981.

[36] Jouvet, B. and Pythian, R.: Quantum aspects of classical statistical fields. *Phys. Rev. A*, vol. 19, pp. 1350 – 1355, 1979.

[37] Martin, P., Siggia, E. and Rose, H.: Statistical dynamics of classical systems. *Phys. Rev. A*, vol. 8, p. 423, 1973.

[38] Fredrickson, G.H.: *The Equilibrium Theory of Inhomogeneous Polymers*. Oxford University Press, Oxford, 2006.

[39] Edwards, S.: A field theory formulation of polymer networks. *J. Phys. (France)*, vol. 49, pp. 1673–1682, 1988.

[40] Deam, R. and Edwards, S.: The theory of rubber elasticity. *Phil. Trans. Roy. Soc. A*, vol. 280, pp. 317–353, 1976.

[41] Mezard, M., Parisi, G. and Virasoro, M.: *Spin Glass Theory and Beyond An Introduction to the Replica Method and Its Applications*. World Scientific Publishing, Singapore, 1987.

[42] Fredrickson, G.H. and Helfand, E.: Collective dynamics of polymer solutions. *J. Chem. Phys.*, vol. 93, no. 3, pp. 2048–2061, 1990.

[43] Touchette, H.: The large deviation approach to statistical mechanics. *Phys. Rep.*, vol. 478, pp. 1–69, 2009.